Title

Interlaboratory Study for Characterizing Monoclonal Antibodies by Top-Down and Middle-Down Mass Spectrometry

Journal

Journal of The American Society for Mass Spectrometry, 31(9)

ISSN

1044-0305

Authors

Srzentić, Kristina
Fornelli, Luca
Tsybin, Yury O
et al.

Publication Date

2020-09-02

DOI

10.1021/jasms.0c00036

Peer reviewed

HHS Public Access

Author manuscript

J Am Soc Mass Spectrom. Author manuscript; available in PMC 2021 September 02.

Published in final edited form as:

J Am Soc Mass Spectrom. 2020 September 02; 31(9): 1783–1802. doi:10.1021/jasms.0c00036.

Interlaboratory Study for Characterizing Monoclonal Antibodies by Top-Down and Middle-Down Mass Spectrometry

A full list of authors and affiliations appears at the end of the article.

Abstract

The Consortium for Top-Down Proteomics (www.topdownproteomics.org) launched the present study to assess the current state of top-down mass spectrometry (TD MS) and middle-down mass spectrometry (MD MS) for characterizing monoclonal antibody (mAb) primary structures, including their modifications. To meet the needs of the rapidly growing therapeutic antibody market, it is important to develop analytical strategies to characterize the heterogeneity of a therapeutic product's primary structure accurately and reproducibly. The major objective of the present study is to determine whether current TD/MD MS technologies and protocols can add value to the more commonly employed bottom-up (BU) approaches with regard to confirming protein integrity, sequencing variable domains, avoiding artifacts, and revealing modifications and their locations. We also aim to gather information on the common TD/MD MS methods and practices in the field. A panel of three mAbs was selected and centrally provided to 20 laboratories worldwide for the analysis: Sigma mAb standard (SiLuLite), NIST mAb standard, and the therapeutic mAb Herceptin (trastuzumab). Various MS instrument platforms and ion dissociation techniques were employed. The present study confirms that TD/MD MS tools are available in laboratories worldwide and provide complementary information to the BU approach that can be crucial for comprehensive mAb characterization. The current limitations, as well as possible solutions to overcome them, are also outlined. A primary limitation revealed by the results of the present study is that the expert knowledge in both experiment and data analysis is indispensable to practice TD/MD MS.

Graphical Abstract

Corresponding Author tsybin@spectroswiss.ch.

†Author Contributions

K.S. and L.F. contributed equally.

Supporting Information

The Supporting Information is available free of charge at https://pubs.acs.org/doi/10.1021/jasms.0c00036.

Details and examples of the experimental results, including tables and figures with information about sample preparation, mass spectrometry, and data analysis methods and techniques employed by the study participants, and the results of the statistical analysis of the measurements performed by the study participants (PDF)

The authors declare the following competing financial interest(s): Anja Resemann, Stuart Pengelley, and Detlev Suckau are employees of Bruker Daltonics, which manufactures TOF MS and FT-ICR MS instruments and commercializes allied software. Anton Kozhinov, Konstantin Nagornov, and Yury Tsybin are employees of Spectroswiss, which develops and commercializes FTMS data processing and data analysis software. Neil Kelleher is involved with commercialization of ProSight software for data analysis. Paul Danis is also the Founder and Principal of Eastwoods Consulting, providing business advisory services to life science companies.

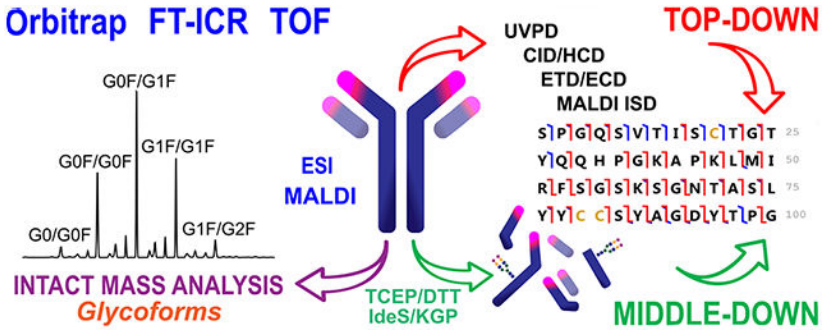

Keywords

Therapeutic protein; glycoform; intact mass measurement; tandem mass spectrometry; MS/MS; Fourier transform mass spectrometry; FTMS

INTRODUCTION

The complete characterization of protein therapeutics (amino acid sequence, clipping or truncation, glycosylation profiling, disulfide bonding patterns, secondary and higher order structure, etc.)[1] and associated impurities (e.g., host cell proteins) are a major concern for the pharmaceutical and biotechnology industries.[2] The structural characterization of monoclonal antibodies (mAbs), both as therapeutics and as reagents, is an essential part of their production and regulatory approval.[3] It could be envisioned that the in-depth characterization of a protein drug in the future will be as complete and rapid as it is for small molecule drugs today, but there are no standard protocols or technologies (yet). Considering its importance in small molecule characterization, high-performance mass spectrometry is likely to play a prominent role in this endeavor. The recent progress in development, industrial, and regulatory acceptance of the multiattribute method (MAM) that includes MS procedures for mAb characterization is an example.[4-8] MAM has been developed to monitor and quantify the array of post-translational modifications (PTMs) found on biotherapeutic molecules during product characterization, in-process control, Good Manufacturing Practice (GMP) release and stability testing steps.[4]

The market for therapeutic proteins, specifically the monoclonal antibody (mAb) market, has significantly increased in the past decade (7–18% growth each year).[9] mAb sales exceeded 98 billion USD as of December 2017 and are to grow to 130–200 billion USD by 2022.[9,10] In 2019 alone, the US Food and Drug Administration (FDA) Center for Drug Evaluation and Research approved three mAbs, ten biosimilars, one nanobody, one single chain Fv (scFv), and three antibody-drug conjugates (ADCs) as drugs (www.antibodysociety.org).[11,12] At least 79 novel antibodies are under investigation in late-stage clinical studies.[13]

Regulatory agencies (e.g., FDA and Pharmacopeia) require thorough characterization of all new drug products before their approval. However, compared to characterizing small molecules, therapeutic mAbs present distinct challenges for the analytical laboratory. In addition to their large size—on the order of 150 kDa for a full-sized mAb—the presence of

post-translational modifications (PTMs), such as glycosylation, oxidation, and deamidation, add to the structural complexity and heterogeneity of mAbs.[14] Such PTMs can be referred to as critical quality attributes (CQAs) and may occur during production, purification, or storage.[15] Because biotherapeutics are primarily produced in recombinant expression systems (i.e., Chinese hamster ovary (CHO) cells), the final product is heterogeneous. Changes in these systems may manifest as variation in number and distribution of proteoforms,[16] alter efficacy and binding characteristics, or be immunogenic.[17] As a result, comprehensive structural characterization, from primary structure to proteoform elucidation of therapeutic mAbs, is essential.[2,3,18,19]

Mass spectrometry (MS) is a powerful tool for protein characterization.[2,20,21] Two major methodologies that are commonly employed in MS-based protein/proteome analysis are top-down (TD) and bottom-up (BU). The BU approach utilizes proteases or chemical means to cleave proteins at backbone sites to generate smaller, more readily ionizable peptides that are then further fragmented in the gas phase via tandem mass spectrometry (MS/MS) to elucidate sequence and delineate the presence of modifications.[22-26] TD MS strategies eschew the use of proteolytic enzymes, providing the intact masses of the molecules being studied, which in turn can determine the presence of multiple proteoforms.[27] MS/MS fragmentation of the intact proteins and large protein subunits can provide amino acid resolution for interpretation of sequence heterogeneity and presence of PTMs.[21,27,28]

Currently, standard workflows for mAb structural characterization are centered around peptide mapping—analysis of trypsin-derived peptides of 0.6–2 kDa size.[4,5] However, this trypsin-based BU approach does not provide 100% sequence coverage for all mAbs. For example, the blockbuster biotherapeutic, Humira (adalimumab, the world's number 1 drug in sales value), has a very long, more than 50 amino acids, sequence stretch without lysine or arginine residues, which are the specific cleavage sites of trypsin. Therefore, this region of adalimumab may remain unaccounted for (invisible) in a trypsin-based BU approach. To achieve complete sequence coverage and improve PTM characterization, a BU approach employing multiple enzymes is usually required. The additional enzymes are selected to provide cleavage specificity or cleavage frequency complementary to that of trypsin. Examples include chymotrypsin, Lys-C, Glu-C, Asp-N, and Sap9.[23,26,29,30] However, alkylation, followed by digestion with trypsin and other enzymes, entails reaction conditions that can increase the likelihood of artifacts, such as amino acid isomerization, deamidation, or oxidation.[26,31]

TD MS-associated technologies have advanced greatly over the past few decades.[32,33] Since the development of electrospray ionization (ESI), advances in TD MS have focused on two areas—instrumentation and fragmentation approaches.[21,34] Advances, such as improved mass accuracy and resolving power, came with the development of mass analyzers, such as the time-of-flight (TOF), Fourier transform ion cyclotron resonance (FT-ICR), and Orbitrap.[35-37] Newer ion activation/dissociation methods such as electron capture/transfer dissociation (ECD, ETD),[38,39] ultraviolet photodissociation (UVPD),[40] and more efficient matrix-assisted laser desorption ionization (MALDI) matrices for in-source decay (ISD) fragmentation[41,42] drastically increase the sequence and PTM information that can be obtained in TD MS experiments. These technological advances have been supported by the

corresponding TD/MD-specific developments in data analysis tools, such as deconvolution of highly convoluted product ion distributions and product ion annotation approaches.[43-47] As a result, TD MS/proteomics has emerged as a powerful tool in basic, translational, and clinical research, not only for protein identification but also for large-scale proteoform elucidation.

Unlike BU approaches, TD MS offers extensive, if not complete, sequence coverage and proteoform mapping in a single experiment, and relies on sample handling protocols minimizing the introduction of artifactual modifications (e.g., oxidation and deamidation). Among other virtues, proteoform mapping provides valuable information on the integrity of a mAb, informing about structural integrity of a whole mAb in solution, which is inherently lost in the BU approach.[48] However, for proteins of 150 kDa size, overall sequence coverage based on current TD MS technologies remains incomplete.[49-53] Therefore, reducing the size of the target proteins through reduction of mAbs into their heavy and light chain (Hc and Lc) subunits is often required to provide more detailed information, Figure 1.[33,54-57]

Furthermore, artifact-minimizing enzymatic processing of intact mAbs into 25–50 kDa subunits by use of structure- specific proteases, for example, IdeS and KGP, has recently received attention.[58-60] Separating mAbs by backbone cleavage above (KGP) or below (IdeS) the hinge region yields a monovalent antigen-binding fragment (Fab) or a bivalent F(ab′)2 subunit, respectively, and a fragment crystallizable (Fc) glycosylated subunit, Figure 1. Further size reduction of large F(ab) and $F(ab')_2$ subunits is typically accomplished with the use of disulfide bond chemical reduction, to yield smaller subunits: Lc, Fd′ (the N-terminal part of an Hc), and Fc/2 (the C-terminal part of an Hc). Chemical reduction of S-S bonds can be performed by use of, for example, TCEP or DTT. Naturally, the number of amino acids in the Fd′ and Fc/2 subunits formed with IdeS or KGP enzymes will be different.

Despite the relatively large size of typical mAb subunits (Lc, Hc, F(ab), Fd′, and Fc/2), enzymatic or chemical separation of an intact mAb into these smaller components for MS-based analysis should be referred to as middle-up (MU) MS, and their MS/MS analysis as middle-down (MD) MS.[27] For example, the combination of MU and MD measurements were previously applied to detect the reference sequence errors and curation of the cetuximab and natalizumab sequences.[33,57] Certain MD proteomics approaches may utilize even more extensive protein cleavage specificity, yielding proteolytic peptides in the range of 3–7 kDa,[25,61,62] as demonstrated for mAbs analysis.[26]

To assess the added-value of the current technologies and protocols offered by TD/MD MS for characterizing mAbs compared to BU MS, the present study was launched and supervised by the Consortium for Top-Down Proteomics (www.topdownproteomics.org). This study engaged 20 laboratories worldwide. All of the groups who volunteered have some level of expertise in TD/MD MS, but several had limited or no experience with 150 kDa mAb proteins. Three commercially available mAbs (SiLuLite mAb, NIST mAb, and trastuzumab, vide infra) were centrally provided to participants. Each group performed TD/MD MS experiments following their own best practices and approaches on all or some of the provided mAbs. A broad range of MS instruments and ion activation/dissociation

techniques was employed. To provide a detailed description of the employed techniques and the results obtained, the current report is supported by Supporting Information. It presents results of data analysis in the form of box-plots (Figures S1-S26) and experimental results (Figures S27-S66), as well as tables with sample information, description of the employed methods and techniques, as well as selected results overview (Tables S1-S16).

Ultimately, the study highlights the current state of TD/MD MS to address the challenges for ensuring the quality of biotechnology medicinal products, their limitations, and where future development is needed. This report and perspective should be of value not only to protein mass spectrometrists who are interested in TD/MD MS and biopharmaceutical scientists currently engaged in characterization of therapeutic proteins but also to students and early career researchers who wish to be educated in the important field of mAb structure characterization.

■ EXPERIMENTAL SECTION

Initial Antibody Sample Preparation.

Three commercially available mAbs (immunoglobulin G or IgG, isotype 1) were provided to participants in equal amounts (from 50 to 100 μg/sample): Sigma mAb standard (SiLuLite, IgG1 lambda, CHO, Sigma); NIST mAb standard (HzIgG1 kappa, NS0, NIST) and Herceptin (trastuzumab, HzIgG1 kappa, CHO, Roche); see Table S1 for mAb sequence information, Table S2 for details about sample preparation and handling, and Table S3 for the results of quality control measurements. Each mAb was provided in three forms for different experimental workflows, Figure 1: (i) intact form for mass measurements and TD analysis of the 150 kDa mAbs; (ii) mAbs digested by use of the highly specific protease KGP (GingisKHAN, Genovis, Lund, Sweden);[63] and (iii) mAbs digested by the IdeS protease (Fabricator, Genovis).[64] In the latter case, the Fc subunit integrity is due to the noncovalent bonds between the two Fc/2 parts. The enzyme/protein ratio for IdeS and KGP digestion corresponded to the manufacturer's suggestions (Genovis). Briefly, one unit of enzyme was added to each microgram of a mAb for IdeS digestion,[58] and two units of enzyme were added to each microgram of a mAb for KGP digestion.[59] Sequence information for each mAb, with the CDR sequences outlined and IdeS/KGP digestion sites highlighted can be found in Table S1. The molecular formulas and calculated masses of modified and unmodified intact mAbs involved in the study and their subunits are presented, together with the details on the atomic masses and abundances employed for the calculations, in Tables S4-S7.

Quality control measurements were performed prior to sample shipping (Table S3 and Figures S27-S29). The samples were shipped on dry ice, after one freeze-thaw cycle, with intact mAbs and their subunits dissolved at high concentration (from 1 to 10 μg/μL in either formulation buffers (intact mAbs) or buffers used for proteolytic digestions (in which case the pH was reduced by addition of formic acid to quench the enzymatic reaction). Note that no reduction of the disulfide bonds was performed before distributing mAbs to participants. The recommended storage conditions were +4 °C for intact mAbs and −20 °C for digests. The participating groups were responsible for sample storage and handling according to their best practices.

Sample Fractionation and Ionization.

Participants were provided the opportunity to decide on the best workflow to purify or separate the intact mAbs and their subunits prior to ionization and TD/MD MS analysis.[34] In most cases, each group used a separation method that they had already established in that laboratory for the types of samples with which they were familiar (Table S8). Groups performing online liquid chromatography (LC) or capillary electrophoresis (CE) coupled with ESI did not typically perform sample cleanup prior to sample fractionation/separation. Conversely, off-line desalting and adduct removal was performed by most groups that were either directly infusing mAb samples (with a syringe or nanoESI needles, or by use of a TriVersa Nanomate robot from Advion BioSciences, Ithaca, NY) or spotting them onto a MALDI plate. The most commonly employed desalting techniques were reversed-phase LC followed by sample collection and solid-phase extraction. Details on the experimental sample preparation (including approaches to disulfide bonds reduction) and fractionation (separation) methods and parameters used by each participant can be found in Table S8.

Mass Spectrometry.

The groups performed TD/MD MS measurements with different instruments, both commercially available and customized (Table S9). The mass analyzers in the present study are TOF, ICR, and Orbitrap FTMS. TOF MS and FT-ICR MS instruments were coupled with either ESI or MALDI ion sources, whereas Orbitrap FTMS instruments used ESI only. Ion activation and dissociation methods coupled to ESI source included: ETD/ECD, higher energy collisional dissociation/collision induced dissociation (HCD/CID), UVPD, MALDI ISD, and a hybrid electron transfer higher-energy collision induced dissociation (EThcD).[65] Instruments were calibrated and maintained by the use of the best laboratory practices specific to each participating group (data not provided). Details on the experimental MS and MS/MS parameters used by participants can be found in Table S9.

Data Analysis.

Complete freedom was left to the participants regarding deconvolution of both nonisotopically and isotopically resolved TD/MD MS spectra, as well as calculation of masses based on known elemental composition and product ion assignment (Table S10). The list of deconvolution algorithms specified by participating laboratories included: Xtract, THRASH, ReSpect (found in both a commercial package from Thermo Scientific and in an open resource as implemented, for example in the MASH Suite), SNAP and MaxEnt (Bruker Daltonics),[66] Intact Mass (Protein Metrics), and UniDec (Oxford University, UK).[67] The list of software used for spectral processing, product ion assignment and validation included the commercially available BioPharma Compass (Bruker Daltonics), ProSight PC and BioPharma Finder (Thermo Scientific), TDValidator (Proteinaceous),[68] Peak-by-Peak and AutoVectis (both from Spectroswiss); and the freeware packages MASH Suite Pro,[45] Informed Proteomics suite,[47] ProSight Lite,[44] and ISDetect.[69] Software tools that bypass deconvolution procedures and perform direct matching of isotopic envelopes of multiply charged productions to simulated profiles included TDValidator, LcMsSpectator (data viewer in Informed Proteomics suite), and AutoVectis. A detailed description of the data processing and analysis tools and parameters employed by participants can be found in

Table S10. Notably, mass tolerance for product ion annotation in MS/MS experiments was typically 10 ppm, and sometimes lowered to 5 ppm. Precursor mass tolerances of up to 50 ppm and 10 Da were reported (Table S10).

For the determination of mass accuracy or mass measurement errors (expressed in parts per million, ppm) from deconvolved full MS measurements, results submitted by the participating laboratories were compared to a single set of calculated masses (determined for both intact mAbs and their subunits). Such masses were calculated by the use of monoisotopic and average atomic masses, as well as abundances, as employed in ChemCalc isotopic calculator algorithm and described elsewhere (Table S4).[70] The respective mAb sequences (Table S1) were used to generate molecular formulas further employed for monoisotopic and average mass calculations of mAbs and their subunits (see examples provided by Tables S5-S7, for data on SiLuLite mAb, NIST mAb, and trastuzumab, correspondingly). These computational results were achieved either with the web-version of ChemCalc (www.chemcalc.org) or via the desktop version of the FTMS Isotopic Simulator (part of Peak-by-Peak software, Spectroswiss). Note that Tables S5-S7 include all major proteoforms identified by participants along with unmodified and deglycosylated proteoforms, some of which were not present in the samples but are given here for didactic and self-controlling reasons. The latter is justified by the errors in molecular weight calculations and proteoform misassignment demonstrated in some reports.

Results of the statistical analysis, in the form of box-and-whisker plots, containing errors (accuracy) for MU and intact mass measurements (Figures S1-S13), as well as sequence coverages (Figure S14-S26), are presented in the Supporting Information. It is important to note that, in all box-and-whisker plots, the box indicates the interquartile range, whereas the horizontal line in the box is the median. All plots were generated by use of R. To perform annotation of glycoforms, this report follows the standard nomenclature, as outlined, for example in a comprehensive report on NIST mAb glycosylation profiling.[71] For tandem MS results, sequence coverage values were obtained directly from the participants' reports, without data reprocessing.

Aggregated Analysis of Results.

A compilation of sample introduction methods, MS and MS/MS instrumentation and allied approaches employed for the study, as reported by the participants, is depicted in Figure 2 and in allied Tables S11 and S12.

The following brief observations could be made (Figure 2 and Tables S11 and S12): (i) most groups employed LC for online sample purification and separation; (ii) about half of the employed instruments were Orbitraps; (iii) most of the currently available MS/MS methods were employed, from a traditional CID to the less frequent but up-and-coming UVPD and MALDI ISD; (iv) most data processing approaches utilized instrument vendor provided software (with some packages requiring additional licenses); and (v) in most cases sequence maps were visualized by use of additional freeware such as the ProSight Lite tool. In general, most groups relied on multiple instruments, activation methods, or data analysis software to characterize the provided mAb samples. We shall note that in the current description we do not separate TD/MD MS results generated with CID (resonant collisional

activation and dissociation performed in ion traps) and HCD (beam-type higher energy collisional activation and dissociation). Further participating group-specific details of the experimental methods are provided in Tables S8-S10.

Bottom-Up Mass Spectrometry.

Standard BU MS approaches, that is, sample handling, mass spectrometry, and data analysis have been employed by several groups, as for example detailed by Smith and co-workers.[72] Details on the employed BU MS approaches, as performed by groups 1, 16, 17, and 24, are given in Tables S8-S10. The corresponding results are summarized in Tables S13 and S15.

■ RESULTS

The following analytical criteria of interest for mAb development, production, quality control, and release have been considered: (i) protein integrity, structure completeness and heterogeneity; (ii) glycoforms, identity and relative quantitation; (iii) protein sequence coverage; (iv) complementarity-determining regions (CDRs) sequencing degree; and (v) other PTM identity and location. These results are reported separately since each of these criteria represents a different level of mAb structural characterization, that is based on different MS methods to achieve the required information (e.g., MS-only versus MS/MS). Another objective of the present study was to evaluate the ease of use and reproducibility of TD/MD MS technologies in current laboratory practice. In this respect, the study aimed to evaluate the maturity of these novel MS approaches in the analytical laboratories performing mAb structure characterization, and potentially widen their acceptance by contract research organizations (CROs), biopharma companies, and proteomics facilities of research institutions.

Protein Structural Integrity.

The structural integrity of mAbs is one of the CQAs in mAb characterization that can reveal potential sources of heterogeneity, including amino acid clipping (truncation) from the C-terminus, modification of N-terminal amino acids, glycosylation, the potential presence of remaining signaling peptides at the N-termini of the Lc and Hc, and overall completeness and stability of mAb's primary structure. Decomposition of an intact mAb into its subunits by chemical and enzymatic digestion, as depicted in Figure 1, facilitates and extends the overall analysis of structural integrity. For example, disulfide bond reduction of a properly assembled intact mAb should result in release of Lc and Hc subunits. The latter may not be the case when mAb structural integrity is not present, which will become apparent by mass measurements of reaction products.

The structural integrity analysis typically starts with mass measurements at the intact mAb level, which is an important part of TD MS workflows.[27,34] Achieving isotopic resolution of intact mAbs today is a challenge that requires the exceptional performance of ultrahigh resolution mass spectrometers.[73,74] It is thus a common practice to perform mass measurements of intact mAbs at a (moderate) resolution sufficient to determine average masses of mAbs' proteoforms.[75] Attention should be paid to the isotopic mass and abundance table employed for calculation of the mAb's average and monoisotopic masses,

which should be listed in corresponding reports (Table S4). For example, average masses for SiLuLite mAb and its subunits as calculated in the current study by use of ChemCalc resource (listed in Table S5) are consistent with the values reported in a follow-up study by Ge and co-workers.[76] A particular benefit of isotopically resolved, and thus higher resolution, mass spectra is disentangling multiple contributions when more than one PTM is present.[76]

Mass measurements of intact mAbs were performed by more than half of the groups participating in this study (Table S12). Overall, the three mAbs analyzed demonstrated excellent protein integrity at the intact mass level, as expected for these samples. Notably, two groups using high-performance FT-ICR MS instruments isotopically resolved the intact mAbs and reported monoisotopic masses. Examples of the FT-ICR mass spectra of the three intact mAbs showing isotopic resolution of the 53+ charge state are shown in Figure S34. To obtain isotopic resolution of these heavy molecules, resolving power exceeding 300 000 at the target *m/z* was achieved by use of a 12 T FT-ICR MS, which correlates with the published results generated with FT-ICR MS or Orbitrap FTMS instruments.[73,74,76] Other groups relied on lower resolution mass spectra that are not isotopically resolved (Figures S30-S33). The average masses of mAbs' proteoforms were obtained from the charge state envelopes generated by ESI MS (Figure 3) or singly or doubly charged components in MALDI MS (data not shown).[77]

To highlight the variation of reported results, the mass measurement errors (expressed in ppm) are presented in this report by both their mean values (Table 1) and their median values. The latter are represented via box-and-whisker plots showing the mass measurement error distributions (Figures S1-S13).

The mass measurement errors achieved through the determination of the monoisotopic mass were not substantially different from those observed for the groups reporting the average intact mAb mass (Figures S1-S3). Indeed, large protein size is known to result in wide isotopic distributions and difficulties in accurately defining monoisotopic masses. In practice, the monoisotopic mass has to be calculated based on statistical methods (e.g., using the averagine approach) that can lead to the associated errors for such large biomolecules.[77] In addition, post-translational modifications (particularly disulfide bonds), incomplete desolvation, and salt adducts (such as sodium) can introduce overlapping isotopic profiles that further complicate the deconvolution and limit the mass accuracy that can be achieved.[78]

To improve the accuracy of their mass measurement, intact mAbs can be broken down into large, 25–100 kDa, subunits by use of enzymatic or chemical sample processing as depicted in Figure 1. The mass measurements of these subunits usually provide results from which Lc (~25 kDa molecular weight) can be isotopically resolved and the monoisotopic mass determined (Figures S7-S13). Isotopic distributions of the larger Hc (~50 kDa) would often remain unresolved and average mass would be reported (Figures S35-S37). Notably, Group 1 reported TOF MS data with monoisotopic masses calculated for both chains, not only for the Lc (see mass assignment method description in Table S10).

The 25 kDa mAb subunits obtained with structure-specific enzymes, similar to the Lc analysis discussed above, are well suited for high-resolution mass measurements.[54,55,58] Examples of MU MS results obtained for NIST mAb analysis with a TOF MS are presented in Figure 4.

Similarly, examples of MU MS results obtained for SiLuLite mAb analysis with Orbitrap FTMS can be consulted in Figure S40. For more details and other examples of experimental results, see Figures S38-S46.

The KGP/IdeS-digested samples were analyzed as provided (unreduced 100 kDa and 50 kDa subunits), or after reduction (and possibly alkylation) of the cysteine residues involved in disulfide bonds to produce three ~25 kDa subunits per mAb, Figure 1. Most of the groups analyzed the reduced subunits, and only one group alkylated the mAb chains, Table S12. As for the Lc and Hc mass measurements, when 25 kDa mAb subunits (Fd′, Fc/2, and Lc) are generated, monoisotopic masses can be derived (Figures S38-S46), but for the 50 kDa subunits both the average and the monoisotopic masses were deduced (Figures S47-S52).

Box-plots showing the mass measurement errors (expressed in ppm) for the subunits derived from mAb digestion with IdeS are shown in Figures S7-S13. Results are summarized for both reduced subunits (25 kDa) and nonreduced subunits (100 and 50 kDa). For instance, Figure S7 shows the box plots for the 25 kDa subunits (derived from all three mAbs) generated by reduction of the IdeS digestion products, aggregated according to the mass analyzer employed. Note that the mass measurement error was typically less than 1–2 ppm for all three mass analyzers when there was no misassignment of the monoisotopic peaks (vide infra), as exemplified by the median values reported in the box-plots. However, the mean mass measurement error calculated from all the reported values, still shows a signification variation, Table 1.

The average mass determination for the nonreduced (50 and 100 kDa, see Figure 1) subunits produced by IdeS digestion (and particularly the ~100 kDa F(ab)2 subunit, which was analyzed only by several groups), was achieved with less than 10 ppm mass measurement error (6.5 ppm for SiLuLite mAb, Figure S13), Table 1. Reduction of intramolecular S–S bonds, if it occurs during IdeS digestion, would result in mass shifts that should be incorporated when average masses are calculated for these large subunits. These mass shifts were not considered in this study for results reported in Figure S13.

Notably, the number of participants that analyzed the ~25 kDa reduced subunits (N = 9 for each antibody, Figures S7-S12) largely exceeds that of the groups that measured the larger, nonreduced subunits and specifically the ~100 kDa F(ab′)2 (N = 4–5 for each antibody, Figure S13), also see Table S12. On one hand, this difference may indicate that the mass measurements of >100 kDa proteins may not be routinely achievable. On the other hand, mass measurements of intact 150 kDa mAbs have been performed by more groups.

Glycoforms: Identity and Relative Quantitation.

N-linked glycans typically represent the most abundant PTMs present in mAbs.[54,76] Because of their important biological and structural role,[79] these complex moieties should be

studied at multiple levels of mAb structural organization.[54] Mass measurements of intact mAbs allow the verification of the pairing of N-linked glycans (i.e., by weighing intact mAb glycoforms or proteoforms), as well as the determination of their relative abundances, Figure 3 and box plots in Figures S4-S13. MU MS is usually more sensitive and accurate than TD MS thanks to a decrease both in protein mass and structural complexity because the sources of heterogeneity (Fd′ and Fc/2 subunits in multiple modified forms) can be decoupled. This approach widens the list of glycans identified (Figures 3 and 4), especially if glycosylation occurs at noncanonical sites (e.g., lysine glycation).[80] Glycation in recombinant mAbs refers to the nonenzymatic addition of monosaccharide (typically a hexose) at free amine groups.[81] Unlike the canonical N-glycosylation, glycation is believed to have minimal effect on target binding, but it contributes to sample heterogeneity and is a necessary target in quality control. Coupled with appropriate molecular mass deconvolution procedures, intact (TD) and MU MS are capable of producing extensive lists of glycoforms (Table S14). Here, we differentiate glycoforms similarly to the standard proteoform notation, for example, the same glycosylation modification on two proteins that differ only by the presence of the C-terminal Lys residue would result in two distinct glycoforms (proteoforms).[16]

Figures S4-S6 show the mass measurement errors for each of the top three glycoforms of the intact mAbs, grouped by mass analyzer employed, namely Orbitrap FTMS, FT-ICR MS, and TOF MS. For example, for SiLuLite mAb, the vast majority of the mass measurements showed accuracy of ≤50 ppm (i.e., ≤8 Da) for each of the three most abundant glycoforms, namely G0F/G0F, G0F/G1F, and G1F/G1F (Figures S5 and S30). In line with these results, MU MS shows that the Hc subunit (Figure S35) and Fc/2 subunit (Figure S41) of SiLuLite mAb are predominantly G0F and G1F modified, with G0 and G2F present also in significant abundance, and with sialylated forms detected at the <1% relative abundance level. These findings are in line with the results of an in-depth TD/MD MS study reported in a recent paper.[76] Similarly, the most abundant glycoforms for NIST mAb and trastuzumab were confirmed in a follow-up TD/MD MS study based on MALDI FT-ICR MS.[82]

Owing to the lower number of participants who reported mass measurement errors for the top three glycoforms of NIST mAb (Figure S4) and trastuzumab (Figure S6), a slightly broader variation in the mass accuracies was reported for the SiLuLite mAb (Figure S5). The latter observation, once again, highlights the importance of advanced training in experimental TD/MD MS. Box-plots showing the errors (expressed in ppm) of glycoform-specific mass measurements for the IdeS-digested and disulfide bond reduced NIST mAb (Figure S9), SiLuLite mAb (Figure S10), and trastuzumab (Figure S11) are displayed by instrument and by proteoform (Supporting Information). A distribution of mass measurement errors for all subunits considered together reported for the most abundant proteoforms, is shown in Figure S12. The reported results indicate that mass measurements errors reported for TOF MS are consistently lower than for the FTMS instruments, Table 1. This rather unexpected result can be rationalized by, presumably, a substantially larger number of participants reporting results for FTMS measurements and in their broader experience level, compared to TOF MS results that were obtained only by high-level experts.

The glycosylation profile revealed by TD/MD MS (Table S14) can be compared with the results generated by the BU MS analysis of short (tryptic) glycopeptides (Table S15) or by

the analysis of isolated glycans prepared by enzymatic removal.[83] A detailed comparison of Tables S14 (TD/MD MS data) and S15 (BU MS data) indicates that differences may be observed between minor glycoforms. For example, BU MS reports a minor, <1% relative abundance, G3F glycosylation for the NIST mAb, which is not reported by TD/MD MS. The latter may indicate that the glycoforms for intact mAbs reported as G1F/G2F, could be instead represented as G0F/G3F glycoforms. Furthermore, BU MS reports Man5 glycosylation for all three mAbs at 1–2% relative abundance. Only a few TD/MD MS reports reported this glycosylation, for example, see Figure 3. Resolving minor glycoforms by TD/MD MS requires optimal operation parameters (e.g., desalting and desolvation), mass resolution, and data processing pipelines. Insufficient resolution/high spectral baseline noise may have rendered the minor glycoforms unreported in many of the TD/MD MS results. For example, results reported in Figure 3 that allowed detection of Man5/Man5 glycoform, have been generated by averaging of unprocessed FTMS data (time-domain transients) from multiple LC-MS technical replicates, see Tables S8-S10 for experimental details.[59]

To evaluate the relative quantitation of major glycoforms, we compared the TD/MD results at the intact mAb, Fc subunit, reduced heavy chain, and Fc/2 levels for the three mAbs. These data are further compared with those obtained at the peptide (BU) level, Figure 5. Overall, the distributions obtained for intact and MU mass measurements match well with those predicted from BU data, in particular for the reduced heavy chain and Fc/2. However, some differences between the intact protein and Fc measurements are observed. In Figure 5a, the simulated profile was overall biased toward lower mass of total glycans compared to the profile measured at the intact protein level (i.e., average fractional abundances of G0F/G1F in NIST, G0F/G0F in SiLuLite, and G0F/G1F in trastuzumab are higher in BU measurements than in intact, and vice versa for G1F/G2F in the three mAbs). The differences between the simulated profile and the experimental data were smaller for Fc (Figure 5b). The same KGP-digested mAb sample also showed that the glycation level on the F(ab) (complementary subunit to Fc as shown in Figure 1) was shown to be 4–7% (standard deviation 1–2%, Table S16), which is higher than the expected level of 1–2% calculated from BU experiments (Table S15).

Assuming no significant loss of glycans during sample processing and ion manipulations, discrepancy in glycosylation levels among different methods may be attributed to two factors. First, ionization efficiencies of glycoforms (large glycoproteins) differ from those of corresponding glycopeptides, and, furthermore, glycosylation may induce changes in digestion efficiency that impacts BU but not intact/MU methods. Second, any potential preferred combinations of glycosylations would invalidate simulated distributions by randomly combining BU data. For example, the G2F/G2F glycoform in intact SiLuLite and G1F/G2F glycoform in trastuzumab (Figure 5a) appeared to be higher than in the simulated values from BU data. It is possible that the chain pairing is preferred between similar glycoforms instead of being purely random (for example, preferentially paring two Hc subunits both with G2F will favor formation of G2F/G2F). Because of limited data in the current study, we could not confirm if the discrepancy seen in Figure 5a is statistically significant. Overall, the distributions from intact/MU measurements were consistent with the simulated values from BU data (assuming random combination), suggesting that chain pairing is largely nonselective. Nonetheless, it is anticipated that such intact and MU

analyses will aid in characterizing chain pairing of bispecific antibodies. The information on PTM combinations cannot be easily retrieved from BU data.[59,84,85]

Amino Acid Sequence Coverage.

Obtaining 100% sequence coverage of mAb primary structure is desired to provide unambiguous and complete characterization.[33,54] In practice, users may define a "100% sequence coverage" for BU and TD/MD approaches differently. It is widely accepted that the BU approach may deliver a 100% sequence coverage of mAbs (often through the use of multiple enzymes and MS/MS methods).[26,29,30,86] That claim assumes that a complete mAb sequence will be confirmed by (overlapping) enzymatically derived peptides. However, not all of these peptides have tandem mass spectra with product ions covering the entire peptide backbone. In the TD/MD MS terminology, a 100% sequence coverage is achieved when protein backbone bonds between *each* pair of amino acids in a protein sequence are cleaved and at least one of the corresponding product ions is detected.[46] In this respect, a complete sequence coverage of mAbs solely by TD or MD approaches has not yet been reported.[53,68] Nevertheless, TD/MD MS provides extensive *sequence information*, which can be instrumental in a mAb characterization strategy when combined with intact mass or BU data or with known mAb structural features (e.g., homologous series and constant regions).[57,87,88] The combination of MS/MS data with accurate mass measurements in TD/MD MS was demonstrated to achieve the required sequence confirmation and even curation in particular cases.[33]

As expected, the highest sequence coverage in this study was obtained by fragmenting the disulfide bond reduced 25 kDa mAb subunits, Figures 6 and S14-S26. Figure 6 shows that, on average, the sequence coverage obtained was 53%, 34%, and 51% for the Lc subunit; 44%, 30%, and 40% for the Fd′ subunit; and 48%, 40%, and 45% for the Fc/2 subunit for NIST, SiLuLite, and trastuzumab mAbs, respectively. The wide range in the reported sequence coverages is due to a few reports that described a sequence coverage as low as 5% from, for example, MALDI ISD. On the other hand, other groups reported substantially higher sequence coverages by use of MALDI ISD, with the maximum sequence coverages among all MS/MS techniques reported for the SiLuLite's Lc subunit (77%), Fd′ subunit (62%), and Fc/2 subunit (87%). Similarly, MALDI ISD yielded the highest sequence coverage for the Fc/2 subunit of trastuzumab (75%). Reporting such a broad distribution for the same MS/MS method may indicate a strong influence of experimental procedures (see Tables S8, S9, and S11). For example, detailed comparison of experimental details provided by groups 1, 15, and 21, which reported MALDI ISD results, suggests that higher sequence coverage of mAb subunits is provided when (i) IdeS digestion is employed together with a complete reduction of intrachain disulfide bonds, (ii) LC is employed to separate the subunits; and, potentially, and (iii) superdihydroxybenzoic acid (sDHB) is employed as a matrix. These conclusions are indicated by results presented in Figures 6 and S22-S24. The added value of point i is further supported by Figures S25 and S26.

Apart from MALDI ISD, the most comprehensive sequence coverage was provided by UVPD (88% for LC subunit of NIST mAb and 89% for the Fc/2 subunit of NIST), and a combination of CID with ETD enhanced by ion–ion proton transfer reactions or PTR (86%

for the Lc subunit and 66% for the Fd' subunit of trastuzumab and 76% for the Fd′ subunit of the NIST mAb). Both MS/MS methods, CID and ETD, were performed in the linear ion trap (LTQ) of the 21 T FT-ICR MS platform.[88] Figure 7 displays the rich tandem mass spectra obtained across a wide *m/z* range generated by the combination of ETD and PTR.

Despite the pronounced simplification of product ion distributions achieved by the PTR approach, which reduces the charge of the product ions to enhance their *m/z* separation, Figure 7 demonstrates a well-resolved but still complex pattern of overlapping isotopic distributions of product ions. Disentangling these product ion contributions can be particularly difficult, as exemplified in the related studies on TD/MD MS of mAbs for diverse MS/MS methods. [49-52,59,68,76,89]

Examples of the sequence maps generated with TD/MD MS approaches in the current study are provided in Figures S60-S66. The total sequence coverage obtained for the ETD/PTR MS/MS data depicted in Figure 7 is one of the highest in the study, Figure 8.

Figure 8 further indicates a certain degree of complementarity in the sequence information obtained between ESI ETD MS/MS and ESI CID MS/MS. Namely, these results report 30 common cleavage sites represented by *c/b* product ions and 25 common sites represented by *z/y* product ions, whereas the number of product ions specific to ETD MS/MS are 81 for *c*-ions and 75 for *z*-ions and those specific to CID MS/MS are 11 for *b*-ions and 11 for *y*-ions. Similarly, integrating data from ESI UVPD MS/MS, MALDI ISD MS/MS, and ESI ETD MS/MS spectra leads to an increased sequence coverage and more confident characterization, Figure 9.

Note that a narrow (a single charge state) or wide (multiple charge states) precursor ion isolation could be performed for ETD MS/MS experiments, whereas there is no precursor ion isolation in MALDI ISD. The latter renders LC separation of mAb subunits prior to MALDI ISD analysis essential. Notably, ETD MS/MS analysis was complementary to MALDI ISD because it frequently extends the coverage of product ions toward the termini. For example, the MALDI ISD product ion ladder from a TOF MS would typically begin with c_8/y_8 or larger product ions, whereas the ETD TOF MS/MS sequence coverage reported here shows the following pattern: (i) Fc/2 subunit, readout from c_2 and (z_4 + 1); (ii) Fd′ subunit, readout from c_2 and (z_2 + 1); and (iii) Lc subunit, readout from c_4 and (z_9 + 1), Figure 10 and Figure 11.

Here, notation "z_n + 1" refers to one of the possible product ion types in ETD MS/MS. Similar observations were reported for MALDI ISD (z_n + 2 type ions) and for ETD MS/MS measurements performed by FT-ICR MS.[82] The "sequence validation percentage", or SVP, approach employed here by group 1 was originally introduced to improve the interpretation of TD/MD sequencing data compared to sequence coverage alone.[33] It uses parametrized conditions to obtain a metric for the percentage of the analyzed sequence that could be validated based on the available data. For example, the SVP method considers sequence gaps as validated if (i) sequence readout starts before or at the 10th (or another user-defined number) amino acid residue from the N- or C- terminus of a given chain, (ii) internal gaps are attributed to Pro-containing moieties, such as …PX… or …PPX…; or (iii) other internal

gaps, say, two amino acid residues long, are immediately followed by an at least equally long sequence tag.[33] Below we describe results from MALDI ISD sequencing, which, although is less common than ETD/CID approaches, has demonstrated promise for mAb analysis.[33,57,82,84]

The LC-free MALDI ISD approach applied to an intact mAb leads to a tandem mass spectrum integrating ISD mass spectra from both mAb Hc and Lc chains. Typically, amino acid readouts are shorter compared to the off-line LC-separated IdeS/KGP-derived subunits and no Fc glycosylation is covered by this approach. In the current study, MALDI ISD performed by off-line LC separation in conjunction with MALDI-TOF MS yielded sequence coverage typically exceeding 70% for all subunits, with the highest value for the Lc of SiLuLite mAb being ~87%; Figures 10 and S62.

The analysis of the trastuzumab, SiLuLite, and NIST mAb Fc/2 subunits yielded 75/77/77% sequence coverage, respectively, in addition to Fd′ 58/62/71%, and Lc 77/87/77%. Thus, an average sequence coverage of 74 ± 8% was observed in the three analyses from LC-MALDI ISD as reported by group 1. For example, as a result of LC-MALDI ISD sequencing of the NIST mAb IdeS-derived subunits, up to 80–100 residues from both the N- and C-termini toward the subunit center were confirmed (Figure 10). Generally, ~7–10 terminal residues were not directly observed in the low-mass background region in MALDI ISD mass spectra. The match was considered as valid (match rules were parametrized in BioPharma Compass software)[33] if the downstream product ions were consistently observed, as detailed above for the rules employed by the SVP approach. In the case of SiLuLite mAb, the Lc subunit was largely sequenced, with the only gap between residues 109–113. Similarly, for the Fd′ subunit, sequence was largely confirmed, except for residues between positions 89–147. However, for both Lc and Fd′, additional modifications or sequence variations can be excluded based on the mass measurements, which all agree with the calculated masses of the fully reduced subunits. In the case of the Fc/2 subunit, the sequence was confirmed for the C-terminus lysine-loss proteoform (lysine clipping). Residues 98–124 were not directly covered, and thus modifications/sequence variations in this region could not be ruled out. However, as for Lc and Fd′ subunits, the complementary intact and MU MS data are in agreement with the absence of such variations. These MALDI ISD TOF MS sequencing results can be compared with the follow-up report that employed a higher-resolution MS instrument, namely, 12 T FT-ICR MS.[82]

CDRs Sequencing.

CDRs represent the variable domains of mAbs. They contribute to the unique antigen-binding properties of mAbs, distinguishing various mAbs from each other.[54] As a result, complete sequencing of CDRs is one of the CQAs for mAb structural analysis. The mAbs considered here are of the IgG1 isotype and thus each of them has three CDRs in both the Lc and Hc subunits (Table S1).

BU MS is currently the method of choice for CDR sequencing.[29] It can provide 100% sequence coverage of all CDRs, especially if de novo sequencing is not needed, as was the case with the present study. To obtain benchmarking results, three groups participating in the current study were tasked to perform BU MS in addition to TD/MD MS approaches. For the

three mAbs employed in this study, a conventional BU approach provided 100% sequence coverage for all CDRs. For example, group 16 obtained 100% sequence coverage for all CDRs in all three mAbs by employing Lys-C for digestion. Group 24 employed a mixture of 3 enzymes (trypsin, Glu-C, and chymotrypsin) to digest the mAbs and obtained 100% sequence coverage for all CDRs except one (CDR3 in the NIST mAb Hc).

TD/MD MS sequencing of CDRs follows the same pattern described for general sequencing: the Lc CDRs were on average better covered than those belonging to the Fd′ (or the Hc). In particular, CDR3 of the Fd′ was sometimes poorly covered; for example, group 10 reported zero backbone bonds cleaved for trastuzumab's CDR3 and only one backbone bond cleaved for the NIST mAb's CDR3 based on the MD MS/MS of mAb subunits with an Orbitrap FTMS platform. Conversely, the CDR1 and CDR2 of trastuzumab and NIST mAb were on average characterized with ~50% of the bonds cleaved, as reported by the same group. Group 8 employed a 21 T FT-ICR MS to extensively sequence mAb subunits, with mass spectral data and sequence coverage map examples shown in Figures 6 and 7, respectively. With regard to the CDR coverage reported in Figure 8 for the Lc of SiLuLite mAb, a total of 11 bonds out of 13 were cleaved for CDR1, 5 out of 6 for CDR2 and all bonds were cleaved for CDR3. LC-MALDI ISD TOF MS of the reduced NIST mAb (Lc + Hc mixture) sequenced four out of six CDRs (group 1). When the same approach was applied to the IdeS-derived subunits of NIST mAb, five out of six CDRs were confirmed with relatively high, >85%, sequence coverage for 3 CDRs on the Lc and 2 CDRs on the Fd' domain (Figure 11). In summary, together with the achievable low ppm mass accuracy for mass measurements of mAb subunits (IdeS digestion followed by disulfide bond reduction), the combination of both MD and BU approaches leaves little uncertainty about the correctness of the given sequence in general and of CDRs in particular.

The CDRs of the Hc and Lc subunits were similarly covered and highly sequenced with MALDI ISD implemented on a 15 T FT-ICR MS, Figures 9 and S66. Briefly, the following results were reported: for the Hc subunit, 100% (8 out of 8 bonds cleaved) sequence coverage of CDR1, 88% (7 out of 8 bonds cleaved) sequence coverage of CDR2, and 86% (12 out of 14 bonds cleaved) sequence coverage of CDR3; and for the Lc subunit, 100% (8 out of 8 bonds cleaved) for CDR1, 83% (5 out of 6 bonds cleaved) for CDR2, and 78% (7 out of 9 bonds cleaved) for CDR3.

Overall, sequence analysis of the 50 kDa subunits of trastuzumab based on MALDI ISD MS/MS shows that the CDR coverage follows what was also observed for the disulfide-protected Lc and Fd′ subunits obtained by IdeS proteolysis. The MS/MS analysis of the larger subunits, for example, 100 kDa F(ab′)2 subunits generated by IdeS proteolysis without disulfide bond reduction, shows the importance of high order structure (retained in the gas phase mainly due to the presence of disulfide bridges) for any MS/MS approach employed.[51] These results are rationalized by considering that the CDR3 is located in the disulfide-free loop approximately at the center of each F(ab′)2 chain, and correlates with the prior reports on TD MS of intact mAbs.[49-51]

■ DISCUSSION

Performance Evaluation of Middle/Top-Down Approaches.

The results reported above demonstrate an overall correlation between the analytical performance and mAb structural information obtained here and the TD/MD MS reports published to date (see Introduction). The mass measurements of intact mAbs and their subunits are critical in providing knowledge on the mAb structural integrity, a feature which cannot be directly revealed by BU approaches.

This study further emphasizes that care should be taken when calculating molecular weights of mAbs and their subunits. In particular, these calculations have to take into account the state (oxidized or reduced) of all disulfide bonds (Tables S5-S7). The risk of misassignments of the monoisotopic peak for 50–100 kDa subunits increases compared to 25 kDa subunits. Misassignment can increase the mass errors by multiples of about ±1 Da.[45] Furthermore, peak interferences due to partially reduced mAb subunits are common and should be prevented by thorough reduction methods or considered during data analysis.[33] The molecular weight determination of 25 kDa mAb subunits can drastically reduce this shortcoming, as seen with the IdeS or KGP approach (with disulfide bond reduction) and the disulfide-bond reduced mAb data set analysis. However, even monoisotopic mass measurements of 25 kDa based on state-of-the-art MS instruments can provide mass measurement errors exceeding 10 ppm (Figure S7). Among the origins for these errors are (i) incomplete reduction of disulfide bonds of intact mAbs or mAb subunits after IdeS/KGP digestion, (ii) misassignment of monoisotopic mass upon deconvolution,[45] and (iii) reporting of average mass instead of monoisotopic mass. Let us consider these sources of errors in more detail.

Several proteoforms of mAb subunits exhibiting a different number of oxidized/reduced disulfide bonds can often be observed in the same MU/MD MS experiment. Therefore, the appropriate precursor ion mass needs to be considered for peak annotation (Tables S5-S7). In the current study, most of the groups reported monoisotopic masses of 25 kDa mAb subunits in which all disulfide bonds were reduced. Fewer groups reported results for precursor ions with all (two) disulfide bonds intact (mass difference of about 4 Da). One group reported results for subunits with a single intact disulfide bond (mass difference of 2 Da). Once the precursor mass was corrected for an appropriate number of disulfide bonds reduced/oxidized, the mass measurement errors were generally within 1–2 ppm (Figure S7). However, the reported results demonstrate high variation of the mass measurement errors, significantly increasing the mean mass measurement errors even for high-performance FTMS instruments, Table 1. The misassignment of a monoisotopic mass as a result of the deconvolution procedure remains a common problem. The submitted results exhibited both 1 and 2 Da shifts toward lighter or heavier experimentally obtained masses, which resulted in significant mass measurement errors. These errors could be due to erroneous outcomes of deconvolution algorithms applied to statistically poorly represented isotopic envelopes of multiply charged protein precursor ions.

For glycan profiling, the general approach was to measure the masses of the intact mAb or IdeS/KGP-digested mAbs, with or without disulfide bond reduction. The difference between

the expertise levels of participants was apparent: a few groups were able to provide more information on intact proteoforms than just the typical N-linked glycosylation, C-terminal Lys clipping, or N-terminal formation of pyroglutamate (pyro-Q or pyro-E). Subunit-level glycoform profiling brings an additional benefit of separating the Fc/2 subunit with the expected N-linked glycosylation from the Fd′ and Lc subunits. This profiling aids in confirming the expected modifications or revealing unexpected glycosylation modifications on other than the Fc/2 subunits.[57] In the mAb samples employed in the current study, most of the glycosylation modifications are located in the conserved site on Fc/2, whereas glycation sites (Hex) were detected in the Lc and Fd′ at a few percent by MU and BU experiments (Tables S15 and S16). The latter is normally related to the use of enzymes, for example, EndoS or IgGZERO, for removing the glycans during sample preparation.[90] Similarly, it is also known that the integrated BU and MU approach can be useful in detecting O-HexNAc modification in the hinge region of some mAbs, which was not the case here.[91,92]

The reported maximum sequence coverages for diverse MS/ MS methods for both TD and MD MS/MS approaches correlate well with the current literature on this subject. For example, in addition to ETD with PTR and multiple fills of the C-trap (Figure S57), one of the higher sequence coverages was obtained by 193 nm UVPD for the reduced Fc/2 subunit of the NIST mAb (89%) performed with an Orbitrap FTMS instrument (Figure S61). Different ion activation methods have shown a good degree of complementarity for the characterization of mAb subunits (see fragmentation maps integrating CID and ETD in Figure 8, as well as UVPD, ETD, and MALDI ISD in Figure 9).

Overall, TD/MD MS results are reliable if a significant length of sequence tag, more than 2–3 amino acids, is obtained, and they are further strengthened by complementary product ions (from both ends of a protein sequence). Individually matching product ions, ones that do not form sequence tags with other product ions, are questionable and may not be suitable to confirm or reject sequence assignments. It is apparent that achieving maximum sequence coverages necessitates a high level of expertise in TD/MD MS/MS practice, which was reflected by the wide spread of sequence coverages reported here (Figures S14-S26). Nevertheless, the results of this study show that achieving complete sequence coverage for all CDRs for the same mAb by use of TD/MD MS even by the expert users was not always possible (Figures 7-9).

The strength of the 50–100 kDa subunit mass measurement approach perhaps lies not so much in the best possible accuracy of the mass determination but in its ability to provide chain pairing information via linking Lc and Fd′ subunits to each other, among other uses.[59] Clearly, MS/MS data obtained from these larger 50–100 kDa disulfide bond-linked subunits are less suitable for full sequence confirmation but can be useful to assess subunit extremities. On the other hand, these conclusions could be a consequence of the fact that, as shown by this study, TD/MD MS analysis of these larger subunits is not as widely practiced by the participating laboratories as intact mAb or smaller subunit analysis. Nevertheless, the large mAb subunits may provide information complementary to intact mass measurements and to MS/MS data, for example when obtaining smaller subunits is prohibited because of sample stability not supporting additional sample processing.

An equally formidable challenge is the identification and assignment of the anticipated dozens or hundreds of internal ions (i.e., fragment ions that do not contain the known N- or C-terminus of the protein) in the MS/MS spectra. Not only are these ions difficult to assign, but they also have the potential to increase the false discovery rate and congest the already dense mass spectra created upon fragmentation of subunits or intact proteins. Despite these hurdles, internal ions could offer an additional rich source of structural information if their data content could be mined.[93,94]

For PTM analysis, MD and TD MS may complement BU MS results and increase the confidence in their identification by deciphering their origins (i.e., sample preparation vs naturally occurring) and their relative stoichiometry. Overall, the modifications observed for the three mAbs were among the most commonly detected in all mAbs-Lys clipping, N-terminal pyro-Glu, and N-linked glycosylation. TD/MD MS revealed Lys clipping on the C-termini of both trastuzumab and NIST mAb, with about 3.1–3.4% glycation of the Lc of SiLuLite mAb. The Fc/2 subunits of all mAbs expectedly contained the truncated glycans resulting from the IgGZERO digestion (deglycosylation) at Asn300 (Asn61 after IdeS digestion, see Table S1).

The selected mAbs represent the three possible cases for pyroglutamate formation at the N-terminus. The two amino acids that can spontaneously cyclize when present at the N-terminus are glutamic acid (Glu) and glutamine (Gln). In the mAbs targeted in the present study, SiLuLite mAb contains both Gln on the N-terminus of the Lc and Glu on the N-terminus of the Hc; whereas NIST mAb has a Gln on the N-terminus of the Hc and trastuzumab has a Glu on its Hc (Table S1). The results reported here allowed for the assignment of all three mAbs to their corresponding incidence of pyro-Glu/Gln modification. Clearly, pyro-Gln (or pyro-Q) formation was present in significantly higher amounts compared to pyro-Glu (pyro-E) modification. For example, the Lc of SiLuLite mAb was found to be about 94% pyroglutamylated (pyro-Q). The calculated masses with pyro-Glu and pyro-Gln modifications for intact mAbs and their subunits are listed in Tables S5-S7.

■ FURTHER CONSIDERATIONS AND OUTLOOK

On the basis of the reports obtained in the present study and from the literature, the current set of conventional approaches for mAb characterization entails (Figure 2 and Tables S11 and S12): (i) sample introduction and ionization, direct ESI infusion or MALDI sample deposition, online LC-MS and LC-MS/MS with ESI or LC-MALDI ISD, or off-line LC-MS and LC-MALDI ISD; (ii) mass spectrometry, MS and MS/MS following the best practices in the corresponding methods and techniques, with use of a single MS/MS method in its conventional implementation (vide infra); and (iii) data processing, deconvolution of MS and MS/MS data for further data analysis. As a few reports have demonstrated, this set of approaches can be efficiently complemented with advanced methods to deliver increased performance, including greater sequence coverage.

The following advanced methods appear to be of particular interest, and could be more widespread in the future: (i) sample introduction and ionization, providing complementary

solution-phase separation of proteins using capillary electrophoresis (CE); (ii) mass spectrometry, increasing population of product ions by multiple fills of the external ion traps (such as the C-trap in Orbitraps), gas-phase fractionating of overlapping ion populations using ion mobility, spreading the condensed product ion distribution in a wider mass range by use of gas-phase ion–ion PTR to reduce the average charge state of product ions (see Figure 7),[95,96] unfolding precursor ions to facilitate product ion separation via precursor ion activation,[97] and considering complementary and chimeric product ion data obtained from multiple MS/MS methods or from the same MS/MS method performed with different experimental parameters; and (iii) data processing, assigning isotopic envelopes of product ions without mass spectra deconvolution and increasing sensitivity and dynamic range via averaging unreduced data from LC-MS/MS technical replicates.[51,59] These advanced approaches aim to reduce the complexity of both mAb precursor and tandem mass spectra by an improved solution-phase and gas-phase fractionation, accompanied by increased sensitivity via enhancing the number of precursor and product ions or by acquiring more data. All of the approaches mentioned above have been employed by the participants of the present study but only by 1–2 groups in each case. Therefore, wider distribution and acceptance of these advanced methods has yet to be achieved.

A more viable combination of MS methods for mAb analysis today in many laboratories is afforded by a conventional BU CID/HCD-based approach (with trypsin, complemented by chymotrypsin digestion, if needed) integrated with intact mAb measurements and MU MS of mAb subunits produced by IdeS digestion and disulfide bond reduction.[98] To provide sequencing and PTM information on mAbs, the complementarity of MS/MS methods suggests usage of a CID-type method, for example, HCD, with a radical-chemistry driven MS/MS approach, for example, ETD, EThcD, or UVPD. Adding MALDI ISD sequencing appears to be attractive for mAb analysis. Potentially, a single MS platform should be able to perform efficient BU, MD (for example with IdeS and other enzymes) and intact mass measurement on whole mAbs (low resolution) and MU on subunits (high resolution). However, based on the experience of this project, this strategy is not trivial. Standardization of reporting and data analysis software is necessary. If BU data and TD/MD MS data can be more effectively integrated, some of the lower magnitude peaks in TD/MD mass spectra will be more proficiently assigned. In turn, this integration will inform how the pieces detected in BU assemble as a whole. Therefore, further software development is needed to enable data integration. For example, group 17 performed extensive BU MS studies of SiLuLite, employing four enzymes and two different MS/MS methods, HCD and ETD (Table S13). Nevertheless, they were not able to provide 100% sequence coverage for the Hc of SiLuLite, even by combining sequencing information from all four employed enzymes and despite applying advanced bioinformatics approaches.[72] A completely unsequenced region was found to be part of a Hc above the hinge region with the sequence DYFPEPVTVSW. On the other hand, MD MS data for the same sequence region of SiLuLite performed on the Fd′ subunit show complete sequence coverage of this region (see, for example, Figure S5 in a report by Ge and co-workers).[76] Therefore, integration of BU MS and MD MS data could provide 100% sequence coverage for SiLuLite mAb. Interestingly, BU MS-derived 100% sequence coverage for the Hc subunit was reported only by one group and only for trastuzumab (Tables S13 and S15).

In the present study, many of the figures submitted by the participants displayed manually annotated mass spectra, which indicates that an extensive effort is still required to derive structural conclusions from raw data. Automation of data analysis with no loss in accuracy is evolving with the recent developments of both open source and commercial software workflows for biopharma applications.[33] Recent advancements in algorithms for data analysis of protein mass spectra aim at more accurate peak assignment (for accurate monoisotopic or average mass calculation),[99] as well as improved deconvolution of complex product ion mass spectra and attempts to perform de novo TD MS sequencing.[100]

In principle, TD/MD MS could be integrated into the next generation MAM workflows, which presently employ BU-derived methods. TD/MD MS could be beneficial for MAM by reducing labor involved in sample preparation and minimizing the risk of artifacts. In fact, intact mass measurements are already a part of MAM approaches accepted in biopharmaceutical industry, with MU approaches being under evaluation.[7] For these approaches to be fully accepted, mass tolerance settings (e.g., <0.3 Da or <12 ppm at 25 kDa) could be used as analytical criteria to reliably distinguish target mAb structures from, for example, deamidated species. Nevertheless, extensive efforts to increase sample throughput of TD/MD MS, automate data acquisition, and develop specialized software are needed to integrate the full capabilities of TD/MD MS into MAM workflows. Standard reference materials, such as the commercially available and analyzed here NIST and SiLuLite mAbs, can be used to establish system suitability that is similarly required for regulatory approval of BU analysis.[101]

■ CONCLUSIONS

This comparative interlaboratory study highlights the value of readily available TD/MD MS tools for mAb structural analysis. The wide diversity in the instrumentation and methods employed by the 20 partner laboratories of this project captures the current state of TD/MD MS, that is, there is no “one size fits all.” Compared to the techniques and instruments used for BU, TD/MD, approaches are still very much in development. However, the potential for higher performance protein analysis in the future is clearly apparent as instrumentation capabilities improve, and advanced TD/MD methods become more widely available. Already today, many of the TD/MD tools are accepted by analytical departments in various CROs, pharma/biotech companies, and service facilities in academic institutions worldwide.

Although mAb sequence coverage from MS/MS data is currently less than 100% for either MD or TD MS, information complementary to BU approaches is obtained in a more rapid fashion, which may be crucial or beneficial for comprehensive and unambiguous mAb characterization. Particularly, mass measurements of intact mAbs (part of TD MS) and structural subunits of mAbs (MU MS) are an important complement to BU approaches. On the other hand, the present study also uncovered the wide range of expertise levels found among the participants for TD/MD MS protein characterization. Clearly, there is a need for advanced training of the analytical scientists performing complex MS-based experiments, such as denaturing and native TD/MD MS of mAbs.[27]

Interestingly, less popular compared to the ESI-based approaches nowadays, the MALDI-based ISD fragmentation approach performed on either TOF or FT-ICR MS instruments has demonstrated a particularly attractive efficiency for mAb sequencing.[82] These results may establish the ground-work for the use of MALDI-based methods for mAb structural analysis and lead to the wider acceptance of TD and MD methods in the industrial environment. That would be in-line with the success of another MALDI-based technology, where MALDI TOF MS is routinely used for microorganism identification via intact mass measurements in many hospitals and healthcare organizations worldwide.[102]

As demonstrated by several groups in this study, there is a strong potential for further development of TD/MD MS techniques that would result in their improved sequencing efficiency and wider acceptance. Reported here are extensions of the standard TD and MD methods, including ETD with multiple fills, CID, ETD and UVPD coupled with PTR, and interexperiment averaging of unreduced (raw) multiple LC-MS/MS technical replicates,[59] that can be among the methods available for implementation in routine workflows. Ion activation techniques, such as UVPD and in-beam ECD,[53] could gain wider use for mAb characterization. The arsenal of MS/MS technologies available today may be further extended by the development of novel methods specifically targeting TD MS of large proteins and protein complexes, such as surface induced dissociation (SID)[103] or hydrogen atom attachment to precursor protein ions in the gas phase.[104]

The original wide scope of the present interlaboratory study was to provide a broad overview of the field as currently practiced. Future studies could monitor the progress of TD/MD MS as the technologies advance. Also, follow-up studies could focus on more targeted topics related to TD/MD MS of mAbs, for example ADC analysis.[105-107]

Supplementary Material

Refer to Web version on PubMed Central for supplementary material.

Authors

Kristina Srzentić[†],
Northwestern University, Evanston, Illinois 60208-0001, United States

Luca Fornelli[†],
Northwestern University, Evanston, Illinois 60208-0001, United States

Yury O. Tsybin,
Spectroswiss, 1015 Lausanne, Switzerland

Joseph A. Loo,
University of California-Los Angeles, Los Angeles, California 90095, United States

Henrique Seckler,
Northwestern University, Evanston, Illinois 60208-0001, United States

Jeffrey N. Agar,
Northeastern University, Boston, Massachusetts 02115, United States

Lissa C. Anderson,
National High Magnetic Field Laboratory, Tallahassee, Florida 32310, United States

Dina L. Bai,
University of Virginia, Charlottesville, Virginia 22901, United States

Alain Beck,
Centre d'immunologie Pierre Fabre, 74160 Saint-Julien-en-Genevois, France

Jennifer S. Brodbelt,
University of Texas at Austin, Austin, Texas 78712-1224, United States

Yuri E. M. van der Burgt,
Leiden University Medical Centre, 2300 RC Leiden, The Netherlands

Julia Chamot-Rooke,
Institute Pasteur, 75015 Paris, France

Sneha Chatterjee,
University of Antwerp, 2000 Antwerp, Belgium

Yunqiu Chen,
Biogen, Inc., Cambridge, Massachusetts 02142-1031, United States

David J. Clarke,
The University of Edinburgh, EH9 3FJ Edinburgh, United Kingdom

Paul O. Danis,
Consortium for Top-Down Proteomics, Cambridge, Massachusetts 02142, United States

Jolene K. Diedrich,
The Scripps Research Institute, La Jolla, California 92037, United States

Robert A. D'Ippolito,
University of Virginia, Charlottesville, Virginia 22901, United States

Mathieu Dupré,
Institute Pasteur, 75015 Paris, France

Natalia Gasilova,
Ecole Polytechnique Fédérale de Lausanne, 1015 Lausanne, Switzerland

Ying Ge,
University of Wisconsin-Madison, Madison, Wisconsin 53706, United States

Young Ah Goo,
University of Maryland, Baltimore, Maryland 21201, United States

David R. Goodlett,
University of Maryland, Baltimore, Maryland 21201, United States

Sylvester Greer,
University of Texas at Austin, Austin, Texas 78712-1224, United States

Kim F. Haselmann,
Novo Nordisk, DK-2760 Malov, Denmark

Lidong He,
National High Magnetic Field Laboratory, Tallahassee, Florida 32310, United States

Christopher L. Hendrickson,
National High Magnetic Field Laboratory, Tallahassee, Florida 32310, United States

Joshua D. Hinkle,
University of Virginia, Charlottesville, Virginia 22901, United States

Matthew V. Holt,
Baylor College of Medicine, Houston, Texas 77030-3411, United States

Sam Hughes,
The University of Edinburgh, EH9 3FJ Edinburgh, United Kingdom

Donald F. Hunt,
University of Virginia, Charlottesville, Virginia 22901, United States

Neil L. Kelleher,
Northwestern University, Evanston, Illinois 60208-0001, United States

Anton N. Kozhinov,
Spectroswiss, 1015 Lausanne, Switzerland

Ziqing Lin,
University of Wisconsin-Madison, Madison, Wisconsin 53706, United States

Christian Malosse,
Institute Pasteur, 75015 Paris, France

Alan G. Marshall,
National High Magnetic Field Laboratory, Tallahassee, Florida 32310, United States;
Florida State University, Tallahassee, Florida 32310-4005, United States

Laure Menin,
Ecole Polytechnique Fédérale de Lausanne, 1015 Lausanne, Switzerland

Robert J. Millikin,
University of Wisconsin-Madison, Madison, Wisconsin 53706, United States

Konstantin O. Nagornov,
Spectroswiss, 1015 Lausanne, Switzerland

Simone Nicolardi,
Leiden University Medical Centre, 2300 RC Leiden, The Netherlands

Ljiljana Paša-Tolić,
Pacific Northwest National Laboratory, Richland, Washington 99354, United States

Stuart Pengelley,
Bruker Daltonik GmbH, 28359 Bremen, Germany

Neil R. Quebbemann,
University of California-Los Angeles, Los Angeles, California 90095, United States

Anja Resemann,
Bruker Daltonik GmbH, 28359 Bremen, Germany

Wendy Sandoval,
Genentech, Inc., South San Francisco, California 94080-4990, United States

Richa Sarin,
Biogen, Inc., Cambridge, Massachusetts 02142-1031, United States

Nicholas D. Schmitt,
Northeastern University, Boston, Massachusetts 02115, United States

Jeffrey Shabanowitz,
University of Virginia, Charlottesville, Virginia 22901, United States

Jared B. Shaw,
Pacific Northwest National Laboratory, Richland, Washington 99354, United States

Michael R. Shortreed,
University of Wisconsin-Madison, Madison, Wisconsin 53706, United States

Lloyd M. Smith,
University of Wisconsin-Madison, Madison, Wisconsin 53706, United States

Frank Sobott,
University of Antwerp, 2000 Antwerp, Belgium; University of Leeds, LS2 9JT Leeds, United Kingdom

Detlev Suckau,
Bruker Daltonik GmbH, 28359 Bremen, Germany

Timothy Toby,
Northwestern University, Evanston, Illinois 60208-0001, United States

Chad R. Weisbrod,
National High Magnetic Field Laboratory, Tallahassee, Florida 32310, United States

Norelle C. Wildburger,
Washington University School of Medicine, St. Louis, Missouri 63110, United States

John R. Yates III,
The Scripps Research Institute, La Jolla, California 92037, United States

Sung Hwan Yoon,
University of Maryland, Baltimore, Maryland 21201, United States

Nicolas L. Young,
Baylor College of Medicine, Houston, Texas 77030-3411, United States

Mowei Zhou
Pacific Northwest National Laboratory, Richland, Washington 99354, United States

Affiliations

Northwestern University, Evanston, Illinois 60208-0001, United States

Northwestern University, Evanston, Illinois 60208-0001, United States

Spectroswiss, 1015 Lausanne, Switzerland

University of California-Los Angeles, Los Angeles, California 90095, United States

Northwestern University, Evanston, Illinois 60208-0001, United States

Northeastern University, Boston, Massachusetts 02115, United States

National High Magnetic Field Laboratory, Tallahassee, Florida 32310, United States

University of Virginia, Charlottesville, Virginia 22901, United States

Centre d'immunologie Pierre Fabre, 74160 Saint-Julien-en-Genevois, France

University of Texas at Austin, Austin, Texas 78712-1224, United States

Leiden University Medical Centre, 2300 RC Leiden, The Netherlands

Institute Pasteur, 75015 Paris, France

University of Antwerp, 2000 Antwerp, Belgium

Biogen, Inc., Cambridge, Massachusetts 02142-1031, United States

The University of Edinburgh, EH9 3FJ Edinburgh, United Kingdom

Consortium for Top-Down Proteomics, Cambridge, Massachusetts 02142, United States

The Scripps Research Institute, La Jolla, California 92037, United States

University of Virginia, Charlottesville, Virginia 22901, United States

Institute Pasteur, 75015 Paris, France

Ecole Polytechnique Fédérale de Lausanne, 1015 Lausanne, Switzerland

University of Wisconsin-Madison, Madison, Wisconsin 53706, United States

University of Maryland, Baltimore, Maryland 21201, United States

University of Maryland, Baltimore, Maryland 21201, United States

University of Texas at Austin, Austin, Texas 78712-1224, United States

Novo Nordisk, DK-2760 Malov, Denmark

National High Magnetic Field Laboratory, Tallahassee, Florida 32310, United States

National High Magnetic Field Laboratory, Tallahassee, Florida 32310, United States

University of Virginia, Charlottesville, Virginia 22901, United States

Baylor College of Medicine, Houston, Texas 77030-3411, United States

The University of Edinburgh, EH9 3FJ Edinburgh, United Kingdom

University of Virginia, Charlottesville, Virginia 22901, United States

Northwestern University, Evanston, Illinois 60208-0001, United States

Spectroswiss, 1015 Lausanne, Switzerland

University of Wisconsin-Madison, Madison, Wisconsin 53706, United States

Institute Pasteur, 75015 Paris, France

National High Magnetic Field Laboratory, Tallahassee, Florida 32310, United States; Florida State University, Tallahassee, Florida 32310-4005, United States

Ecole Polytechnique Fédérale de Lausanne, 1015 Lausanne, Switzerland

University of Wisconsin-Madison, Madison, Wisconsin 53706, United States

Spectroswiss, 1015 Lausanne, Switzerland

Leiden University Medical Centre, 2300 RC Leiden, The Netherlands

Pacific Northwest National Laboratory, Richland, Washington 99354, United States

Bruker Daltonik GmbH, 28359 Bremen, Germany

University of California-Los Angeles, Los Angeles, California 90095, United States

Bruker Daltonik GmbH, 28359 Bremen, Germany

Genentech, Inc., South San Francisco, California 94080-4990, United States

Biogen, Inc., Cambridge, Massachusetts 02142-1031, United States

Northeastern University, Boston, Massachusetts 02115, United States

University of Virginia, Charlottesville, Virginia 22901, United States

Pacific Northwest National Laboratory, Richland, Washington 99354, United States

University of Wisconsin-Madison, Madison, Wisconsin 53706, United States

University of Wisconsin-Madison, Madison, Wisconsin 53706, United States

University of Antwerp, 2000 Antwerp, Belgium; University of Leeds, LS2 9JT Leeds, United Kingdom

Bruker Daltonik GmbH, 28359 Bremen, Germany

Northwestern University, Evanston, Illinois 60208-0001, United States

National High Magnetic Field Laboratory, Tallahassee, Florida 32310, United States

Washington University School of Medicine, St. Louis, Missouri 63110, United States

The Scripps Research Institute, La Jolla, California 92037, United States

University of Maryland, Baltimore, Maryland 21201, United States

Baylor College of Medicine, Houston, Texas 77030-3411, United States

Pacific Northwest National Laboratory, Richland, Washington 99354, United States

■ ACKNOWLEDGMENTS

We greatly appreciate the support of the Pilot Project by the Consortium for Top-Down Proteomics and its supporting organizations, Thermo Fisher Scientific, Inc., Bruker Corp., and Genovis AB. We also acknowledge Genovis for providing enzymes (ideS and KGP) and Millipore Sigma for donation of their mAb standard (SiLuLite mAb). J.A.L. acknowledges support from the US National Institutes of Health (R01GM103479, S10RR028893, S10 OD018504); Y.O.T. and J.C.R. from European Horizon 2020 research and innovation program under Grant Agreement No. 829157 (TopSpec); J.S.B. from the Welch Foundation (F-1155) and the National Science Foundation (CHE1402753); YG from NIH GM125085 and S10OD018475; and D.F.H. from the NIH Grant GM037537. L.P.T., J.B.S., and M.Z. acknowledge the support from the Intramural program at Environmental Molecular Sciences Laboratory (EMSL), a DOE Office of Science User Facility sponsored by the Office of Biological and Environmental Research and operated under Contract No. DE-AC05-76RL01830. C.L.H., L.C.A., L.H., and A.G.M. acknowledge support for work performed at the National High Magnetic Field Laboratory, which is supported by National Science Foundation Cooperative Agreement No. DMR-1644779 and the State of Florida. This research was carried out in collaboration with the National Resource for Translational and Developmental Proteomics under Grant P41 GM108569 from the National Institute of General Medical Sciences, National Institutes of Health.

■ REFERENCES

(1). Beck A; Liu H Macro- and Micro-Heterogeneity of Natural and Recombinant IgG Antibodies. Antibodies 2019, 8, 18.

(2). Rathore D; Faustino A; Schiel J; Pang E; Boyne M; Rogstad S The role of mass spectrometry in the characterization of biologic protein products. Expert Rev. Proteomics 2018, 15, 431–449. [PubMed: 29694790]

(3). Taussig MJ; Fonseca C; Trimmer JS Antibody validation: a view from the mountains. New Biotechnol. 2018, 45, 1–8.

(4). Rogers RS; Nightlinger NS; Livingston B; Campbell P; Bailey R; Balland A Development of a quantitative mass spectrometry multi-attribute method for characterization, quality control testing and disposition of biologics. mAbs. 2015, 7, 881–890. [PubMed: 26186204]

(5). Rogers RS; Abernathy M; Richardson DD; Rouse JC; Sperry JB; Swann P; et al. A View on the Importance of "Multi-Attribute Method" for Measuring Purity of Biopharmaceuticals and Improving Overall Control Strategy. AAPS J. 2018, 20, 7.

(6). Xu W; Jimenez RB; Mowery R; Luo H; Cao M; Agarwal N; et al. A Quadrupole Dalton-based multi-attribute method for product characterization, process development, and quality control of therapeutic proteins. mAbs. 2017, 9, 1186–1196. [PubMed: 28805536]

(7). Chen B; Lin Z; Zhu Y; Jin Y; Larson E; Xu Q; et al. Middle-Down Multi-Attribute Analysis of Antibody-Drug Conjugates with Electron Transfer Dissociation. Anal. Chem 2019, 91, 11661. [PubMed: 31442030]

(8). Rogstad S; Yan H; Wang X; Powers D; Brorson K; Damdinsuren B; et al. Multi-Attribute Method for Quality Control of Therapeutic Proteins. Anal. Chem 2019, 91, 14170–14177. [PubMed: 31618017]

(9). Grilo AL; Mantalaris A The Increasingly Human and Profitable Monoclonal Antibody Market. Trends Biotechnol. 2019, 37, 9–16. [PubMed: 29945725]

(10). Walsh G Biopharmaceutical benchmarks 2018. Nat. Biotechnol 2018, 36, 1136. [PubMed: 30520869]

(11). Advancing Health Through Innovation: 2019 New Drug Therapy Approvals by the FDA's Center for Drug Evaluation and Research, 2020 https://www.fda.gov/drugs/new-drugs-fda-cders-new-molecular-entities-and-new-therapeutic-biological-products/new-drug-therapy-approvals-2019.

(12). Duivelshof BL; Jiskoot W; Beck A; Veuthey J-L; Guillarme D; D'Atri V Glycosylation of biosimilars: Recent advances in analytical characterization and clinical implications. Anal. Chim. Acta 2019, 1089, 1–18. [PubMed: 31627805]

(13). Kaplon H; Muralidharan M; Schneider Z; Reichert JM Antibodies to watch in 2020. mAbs. 2020, 12, 1703531. [PubMed: 31847708]

(14). Xu Y; Wang D; Mason B; Rossomando T; Li N; Liu D; et al. Structure, heterogeneity and developability assessment of therapeutic antibodies. mAbs. 2019, 11, 239–264. [PubMed: 30543482]

(15). Nowak CK; Cheung JM; Dellatore S; Katiyar A; Bhat R; Sun J; et al. Forced degradation of recombinant monoclonal antibodies: A practical guide. mAbs 2017, 9, 1217–1230. [PubMed: 28853987]

(16). Smith LM; Kelleher NL; The Consortium for Top Down Proteomics. Proteoform: a single term describing protein complexity. Nat. Methods 2013, 10, 186. [PubMed: 23443629]

(17). Ebbers HC; Crow SA; Vulto AG; Schellekens H Interchangeability, immunogenicity and biosimilars. Nat. Biotechnol. 2012, 30, 1186. [PubMed: 23222784]

(18). Rogstad S; Faustino A; Ruth A; Keire D; Boyne M; Park J A Retrospective Evaluation of the Use of Mass Spectrometry in FDA Biologics License Applications. J. Am. Soc. Mass Spectrom 2017, 28, 786–794. [PubMed: 27873217]

(19). Ambrogelly A; Gozo S; Katiyar A; Dellatore S; Kune Y; Bhat R; et al. Analytical comparability study of recombinant monoclonal antibody therapeutics. mAbs. 2018, 10, 513–538. [PubMed: 29513619]

(20). Aebersold R; Agar JN; Amster IJ; Baker MS; Bertozzi CR; Boja ES; et al. How many human proteoforms are there? Nat. Chem. Biol. 2018, 14, 206–214. [PubMed: 29443976]

(21). Fornelli L; Toby TK; Schachner LF; Doubleday PF; Srzentić K; DeHart CJ; et al. Top-down proteomics: Where we are, where we are going? J. Proteomics 2018, 175, 3–4. [PubMed: 28188863]

(22). Boutz DR; Horton AP; Wine Y; Lavinder JJ; Georgiou G; Marcotte EM Proteomic Identification of Monoclonal Antibodies from Serum. Anal. Chem 2014, 86, 4758–4766. [PubMed: 24684310]

(23). Miller RM; Millikin RJ; Hoffmann CV; Solntsev SK; Sheynkman GM; Shortreed MR; et al. Improved Protein Inference from Multiple Protease Bottom-Up Mass Spectrometry Data. Journal of Proteome Research. 2019, 18, 3429–3438. [PubMed: 31378069]

(24). Cheung WC; Beausoleil SA; Zhang X; Sato S; Schieferl SM; Wieler JS; et al. A proteomics approach for the identification and cloning of monoclonal antibodies from serum. Nat. Biotechnol 2012, 30, 447–452. [PubMed: 22446692]

(25). Srzentić K; Zhurov KO; Lobas AA; Nikitin G; Fornelli L; Gorshkov MV; et al. Chemical-Mediated Digestion: An Alternative Realm for Middle-down Proteomics? Journal of Proteome Research. 2018, 17, 2005–2016. [PubMed: 29722266]

(26). Srzentić K; Fornelli L; Laskay ÜA; Monod M; Beck A; Ayoub D; et al. Advantages of extended bottom-up proteomics using Sap9 for analysis of monoclonal antibodies. Anal. Chem 2014, 86, 9945–9953. [PubMed: 25207962]

(27). Lermyte F; Tsybin YO; O'Connor PB; Loo JA Top or Middle? Up or Down? Toward a Standard Lexicon for Protein Top-Down and Allied Mass Spectrometry Approaches. J. Am. Soc. Mass Spectrom 2019, 30, 1149. [PubMed: 31073892]

(28). McLafferty FW; Breuker K; Jin M; Han X; Infusini G; Jiang H; et al. Top-down MS, a powerful complement to the high capabilities of proteolysis proteomics. FEBS J. 2007, 274, 6256–6268. [PubMed: 18021240]

(29). Sen KI; Tang WH; Nayak S; Kil YJ; Bern M; Ozoglu B; et al. Automated antibody de novo sequencing and its utility in biopharmaceutical discovery. J. Am. Soc. Mass Spectrom 2017, 28, 803–810. [PubMed: 28105549]

(30). Morsa D; Baiwir D; La Rocca R; Zimmerman TA; Hanozin E; Grifnée E; et al. Multi-Enzymatic Limited Digestion: The Next-Generation Sequencing for Proteomics? Journal of Proteome Research. 2019, 18, 2501. [PubMed: 31046285]

(31). Müller T; Winter D Systematic Evaluation of Protein Reduction and Alkylation Reveals Massive Unspecific Side Effects by Iodine-containing Reagents. Mol. Cell. Proteomics 2017, 16, 1173–1187. [PubMed: 28539326]

(32). Toby TK; Fornelli L; Kelleher NL Progress in top-down proteomics and the analysis of proteoforms. Annu. Rev. Anal. Chem 2016, 9, 499–519.

(33). Resemann A; Jabs W; Wiechmann A; Wagner E; Colas O; Evers W; et al. Full validation of therapeutic antibody sequences by middle-up mass measurements and middle-down protein sequencing. mAbs. 2016, 8, 318–330. [PubMed: 26760197]

(34). Donnelly DP; Rawlins CM; DeHart CJ; Fornelli L; Schachner LF; Lin Z; et al. Best practices and benchmarks for intact protein analysis for top-down mass spectrometry. Nat. Methods 2019, 16, 587–594. [PubMed: 31249407]

(35). Loo J; Edmonds C; Smith R Primary sequence information from intact proteins by electrospray ionization tandem mass spectrometry. Science 1990, 248, 201–204. [PubMed: 2326633]

(36). Loo JA; Edmonds CG; Smith RD Tandem mass spectrometry of very large molecules: serum albumin sequence information from multiply charged ions formed by electrospray ionization. Anal. Chem 1991, 63, 2488–2499. [PubMed: 1763807]

(37). Han X; Jin M; Breuker K; McLafferty FW Extending top-down mass spectrometry to proteins with masses greater than 200 kDas. Science 2006, 314, 109–112. [PubMed: 17023655]

(38). McLafferty FW; Horn DM; Breuker K; Ge Y; Lewis MA; Cerda B; et al. Electron capture dissociation of gaseous multiply charged ions by Fourier transform ion cyclotron resonance. J. Am. Soc. Mass Spectrom 2001, 12, 245–249. [PubMed: 11281599]

(39). Syka JEP; Coon JJ; Schroeder MJ; Shabanowitz J; Hunt DF Peptide and protein sequence analysis by electron transfer dissociation mass spectrometry. Proc. Natl. Acad. Sci. U. S. A 2004, 101, 9528–9533. [PubMed: 15210983]

(40). Brodbelt JS Photodissociation mass spectrometry: new tools for characterization of biological molecules. Chem. Soc. Rev 2014, 43, 2757–2783. [PubMed: 24481009]

(41). Demeure K; Quinton L; Gabelica V; De Pauw E Rational Selection of the Optimum MALDI Matrix for Top-Down Proteomics by In-Source Decay. Anal. Chem 2007, 79, 8678–8685. [PubMed: 17939742]

(42). Fukuyama Y; Iwamoto S; Tanaka K Rapid sequencing and disulfide mapping of peptides containing disulfide bonds by using 1,5-diaminonaphthalene as a reductive matrix. J. Mass Spectrom 2006, 41, 191–201. [PubMed: 16382486]

(43). LeDuc RD; Kelleher NL Using ProSight PTM and Related Tools for Targeted Protein Identification and Characterization with High Mass Accuracy Tandem MS Data. Current Protocols in Bioinformatics. 2007, 19, 13.16.11–13.16.28.

(44). Fellers RT; Greer JB; Early BP; Yu X; LeDuc RD; Kelleher NL; et al. ProSight Lite: Graphical software to analyze top-down mass spectrometry data. Proteomics 2015, 15, 1235–1238. [PubMed: 25828799]

(45). Cai W; Guner H; Gregorich ZR; Chen AJ; Ayaz-Guner S; Peng Y; et al. MASH Suite Pro: A Comprehensive Software Tool for Top-Down Proteomics. Mol. Cell. Proteomics 2016, 15, 703–714. [PubMed: 26598644]

(46). Smith LM; Thomas PM; Shortreed MR; Schaffer LV; Fellers RT; LeDuc RD; et al. A five-level classification system for proteoform identifications. Nat. Methods 2019, 16, 939–940. [PubMed: 31451767]

(47). Park J; Piehowski PD; Wilkins C; Zhou M; Mendoza J; Fujimoto GM; et al. Informed-Proteomics: open-source software package for top-down proteomics. Nat. Methods 2017, 14, 909. [PubMed: 28783154]

(48). Nesvizhskii AI; Aebersold R Interpretation of Shotgun Proteomic Data: The Protein Inference Problem. Mol. Cell. Proteomics 2005, 4, 1419–1440. [PubMed: 16009968]

(49). Tsybin YO; Fornelli L; Stoermer C; Luebeck M; Parra J; Nallet S; et al. Structural analysis of intact monoclonal antibodies by electron transfer dissociation mass spectrometry. Anal. Chem 2011, 83, 8919–8927. [PubMed: 22017162]

(50). Mao Y; Valeja SG; Rouse JC; Hendrickson CL; Marshall AG Top-down structural analysis of an intact monoclonal antibody by electron capture dissociation Fourier transform ion cyclotron resonance mass spectrometry. Anal. Chem 2013, 85, 4239–4246. [PubMed: 23551206]

(51). Fornelli L; Ayoub D; Aizikov K; Liu X; Damoc E; Pevzner PA; et al. Top-down analysis of immunoglobulin G isotypes 1 and 2 with electron transfer dissociation on a high-field Orbitrap mass spectrometer. J. Proteomics 2017, 159, 67–76. [PubMed: 28242452]

(52). Fornelli L; Damoc E; Thomas PM; Kelleher NL; Aizikov K; Denisov E; et al. Analysis of intact monoclonal antibody IgG1 by electron transfer dissociation Orbitrap FTMS. Mol. Cell. Proteomics 2012, 11, 1758–1767. [PubMed: 22964222]

(53). Shaw JB; Malhan N; Vasil'ev YV; Lopez NI; Makarov AA; Beckman JS; et al. Sequencing grade tandem mass spectrometry for top-down proteomics using hybrid electron capture dissociation methods in a benchtop Orbitrap mass spectrometer. Anal. Chem 2018, 90, 10819. [PubMed: 30118589]

(54). Zhang Z; Pan H; Chen X Mass spectrometry for structural characterization of therapeutic antibodies. Mass Spectrom. Rev 2009, 28, 147–176. [PubMed: 18720354]

(55). Wang B; Gucinski AC; Keire DA; Buhse LF; Boyne MT II Structural comparison of two anti-CD20 monoclonal antibody drug products using middle-down mass spectrometry. Analyst 2013, 138, 3058–3065. [PubMed: 23579346]

(56). Bondarenko PV; Second TP; Zabrouskov V; Makarov AA; Zhang Z Mass measurement and top-down HPLC/MS analysis of intact monoclonal antibodies on a hybrid linear quadrupole ion trap–Orbitrap mass spectrometer. J. Am. Soc. Mass Spectrom 2009, 20, 1415–1424. [PubMed: 19409810]

(57). Ayoub D; Jabs W; Resemann A; Evers W; Evans C; Main L; et al. Correct primary structure assessment and extensive glyco-profiling of cetuximab by a combination of intact, middle-up, middle-down and bottom-up ESI and MALDI mass spectrometry techniques. mAbs. 2013, 5, 699–710. [PubMed: 23924801]

(58). Fornelli L; Ayoub D; Aizikov K; Beck A; Tsybin YO Middle-Down Analysis of Monoclonal Antibodies with Electron Transfer Dissociation Orbitrap Fourier Transform Mass Spectrometry. Anal. Chem 2014, 86, 3005–3012. [PubMed: 24588056]

(59). Srzentić K; Nagornov KO; Fornelli L; Lobas AA; Ayoub D; Kozhinov AN; et al. Multiplexed Middle-Down Mass Spectrometry as a Method for Revealing Light and Heavy Chain Connectivity in a Monoclonal Antibody. Anal. Chem 2018, 90, 12527–12535. [PubMed: 30252447]

(60). Cotham VC; Brodbelt JS Characterization of Therapeutic Monoclonal Antibodies at the Subunit-Level using Middle-Down 193 nm Ultraviolet Photodissociation. Anal. Chem 2016, 88, 4004–4013. [PubMed: 26947921]

(61). Cristobal A; Marino F; Post H; van den Toorn HWP; Mohammed S; Heck AJR Toward an Optimized Workflow for Middle-Down Proteomics. Anal. Chem 2017, 89, 3318–3325. [PubMed: 28233997]

(62). Laskay ÜA; Srzentić K; Monod M; Tsybin YO Extended bottom-up proteomics with secreted aspartic protease Sap9. J. Proteomics 2014, 110, 20–31. [PubMed: 25123351]

(63). Sjögren J; Andersson L; Mejàre M; Olsson F In Generating and Purifying Fab Fragments from Human and Mouse IgG Using the Bacterial Enzymes IdeS, SpeB and Kgp; Nordenfelt P, Collin M, Eds.; Springer: New York, NY, 2017.

(64). Faid V; Leblanc Y; Bihoreau N; Chevreux G Middle-up analysis of monoclonal antibodies after combined IgdE and IdeS hinge proteolysis: Investigation of free sulfhydryls. J. Pharm. Biomed. Anal 2018, 149, 541–546. [PubMed: 29179100]

(65). Brunner AM; Lössl P; Liu F; Huguet R; Mullen C; Yamashita M; et al. Benchmarking Multiple Fragmentation Methods on an Orbitrap Fusion for Top-down Phospho-Proteoform Characterization. Anal. Chem 2015, 87, 4152–4158. [PubMed: 25803405]

(66). Fornelli L; Parra J; Hartmer R; Stoermer C; Lubeck M; Tsybin YO Top-down analysis of 30–80 kDa proteins by electron transfer dissociation time-of-flight mass spectrometry. Anal. Bioanal. Chem 2013, 405, 8505–8514. [PubMed: 23934349]

(67). Marty MT; Baldwin AJ; Marklund EG; Hochberg GKA; Benesch JLP; Robinson CV Bayesian Deconvolution of Mass and Ion Mobility Spectra: From Binary Interactions to Polydisperse Ensembles. Anal. Chem 2015, 87, 4370–4376. [PubMed: 25799115]

(68). Fornelli L; Srzentić K; Huguet R; Mullen C; Sharma S; Zabrouskov V; et al. Accurate Sequence Analysis of a Monoclonal Antibody by Top-Down and Middle-Down Orbitrap Mass Spectrometry Applying Multiple Ion Activation Techniques. Anal. Chem 2018, 90, 8421–8429. [PubMed: 29894161]

(69). Bakalarski CE; Gan Y; Wertz I; Lill JR; Sandoval W Rapid, semi-automated protein terminal characterization using ISDetect. Nat. Biotechnol 2016, 34, 811–813. [PubMed: 27504771]

(70). Patiny L; Borel A ChemCalc: A Building Block for Tomorrow's Chemical Infrastructure. J. Chem. Inf. Model 2013, 53, 1223–1228. [PubMed: 23480664]

(71). De Leoz MLA; Duewer DL; Stein SE NIST Interlaboratory Study on the Glycosylation of NIST mAb, a Monoclonal Antibody Reference Material, June 2015 to February 2016, NISTIR 8186; NIST, 2017 DOI: 10.6028/NIST.IR.8186.

(72). Li Q; Shortreed MR; Wenger CD; Frey BL; Schaffer LV; Scalf M; et al. Global Post-Translational Modification Discovery. Journal of Proteome Research. 2017, 16, 1383–1390. [PubMed: 28248113]

(73). Valeja SG; Kaiser NK; Xian F; Hendrickson CL; Rouse JC; Marshall AG Unit Mass Baseline Resolution for an Intact 148 kDa Therapeutic Monoclonal Antibody by Fourier Transform Ion Cyclotron Resonance Mass Spectrometry. Anal. Chem 2011, 83, 8391–8395. [PubMed: 22011246]

(74). Shaw JB; Brodbelt JS Extending the Isotopically Resolved Mass Range of Orbitrap Mass Spectrometers. Anal. Chem 2013, 85, 8313–8318. [PubMed: 23909473]

(75). Farrell A; Carillo S; Scheffler K; Cook K; Bones J Monoclonal antibody sequence assessment using a hybrid quadrupole-Orbitrap mass spectrometer. Anal. Methods 2018, 10, 3100–3109.

(76). Jin Y; Lin Z; Xu Q; Fu C; Zhang Z; Zhang Q; et al. Comprehensive characterization of monoclonal antibody by Fourier transform ion cyclotron resonance mass spectrometry. mAbs. 2019, 11, 106–115. [PubMed: 30230956]

(77). Fornelli L; Durbin KR; Fellers RT; Early BP; Greer JB; LeDuc RD; et al. Advancing Top-down Analysis of the Human Proteome Using a Benchtop Quadrupole-Orbitrap Mass Spectrometer. Journal of Proteome Research. 2017, 16, 609–618. [PubMed: 28152595]

(78). Lössl P; Snijder J; Heck AJR Boundaries of Mass Resolution in Native Mass Spectrometry. J. Am. Soc. Mass Spectrom 2014, 25, 906–917. [PubMed: 24700121]

(79). Jennewein MF; Alter G The Immunoregulatory Roles of Antibody Glycosylation. Trends Immunol. 2017, 38, 358–372. [PubMed: 28385520]

(80). Wei B; Berning K; Quan C; Zhang YT Glycation of antibodies: Modification, methods and potential effects on biological functions. mAbs. 2017, 9, 586–594. [PubMed: 28272973]

(81). Li W; Kerwin JL; Schiel J; Formolo T; Davis D; Mahan A et al. Structural Elucidation of Post-Translational Modifications in Monoclonal Antibodies; American Chemical Society, 2015.

(82). van der Burgt YEM; Kilgour DPA; Tsybin YO; Srzentić K; Fornelli L; Beck A; et al. Structural Analysis of Monoclonal Antibodies by Ultrahigh Resolution MALDI In-Source Decay FT-ICR Mass Spectrometry. Anal. Chem 2019, 91, 2079–2085. [PubMed: 30571088]

(83). Nallet S; Fornelli L; Schmitt S; Parra J; Baldi L; Tsybin YO; et al. Glycan variability on a recombinant IgG antibody transiently produced in HEK-293E cells. New Biotechnol. 2012, 29, 471–476.

(84). Gstöttner C; Reusch D; Haberger M; Dragan I; Van Veelen P; Kilgour DPA; et al. Monitoring glycation levels of a bispecific monoclonal antibody at subunit level by ultrahigh-resolution MALDI FT-ICR mass spectrometry. mAbs. 2020, 12, 1682403. [PubMed: 31630606]

(85). Tyshchuk O; Gstöttner C; Funk D; Nicolardi S; Frost S; Klostermann S; et al. Characterization and prediction of positional 4- hydroxyproline and sulfotyrosine, two post-translational modifications that can occur at substantial levels in CHO cells-expressed biotherapeutics. mAbs 2019, 11, 1219–1232. [PubMed: 31339437]

(86). Tran NH; Rahman MZ; He L; Xin L; Shan B; Li M Complete De Novo Assembly of Monoclonal Antibody Sequences. Sci Rep. 2016, 6, 31730. [PubMed: 27562653]

(87). Wu S; Lourette NM; Tolić N; Zhao R; Robinson EW; Tolmachev AV; et al. An Integrated Top-Down and Bottom-Up Strategy for Broadly Characterizing Protein Isoforms and Modifications. Journal of Proteome Research. 2009, 8, 1347–1357. [PubMed: 19206473]

(88). He L; Anderson LC; Barnidge DR; Murray DL; Dasari S; Dispenzieri A; et al. Classification of Plasma Cell Disorders by 21 T Fourier Transform Ion Cyclotron Resonance Top-Down and Middle-Down MS/MS Analysis of Monoclonal Immunoglobulin Light Chains in Human Serum. Anal. Chem 2019, 91, 3263–3269. [PubMed: 30801187]

(89). Shaw JB; Liu W; Vasil′ev YV; Bracken CC; Malhan N; Guthals A; et al. Direct Determination of Antibody Chain Pairing by Top-down and Middle-down Mass Spectrometry Using Electron Capture Dissociation and Ultraviolet Photodissociation. Anal. Chem 2020, 92, 766–773. [PubMed: 31769659]

(90). Sjögren J; Cosgrave EFJ; Allhorn M; Nordgren M; Björk S; Olsson F; et al. EndoS and EndoS2 hydrolyze Fc-glycans on therapeutic antibodies with different glycoform selectivity and can be used for rapid quantification of high-mannose glycans. Glycobiology 2015 25, 1053–1063. [PubMed: 26156869]

(91). Plomp R; Dekkers G; Rombouts Y; Visser R; Koeleman CAM; Kammeijer GSM; et al. Hinge-Region O-Glycosylation of Human Immunoglobulin G3 (IgG3). Mol. Cell. Proteomics 2015, 14, 1373–1384. [PubMed: 25759508]

(92). Zauner G; Selman MHJ; Bondt A; Rombouts Y; Blank D; Deelder AM; et al. Glycoproteomic Analysis of Antibodies. Mol. Cell. Proteomics 2013, 12, 856–865. [PubMed: 23325769]

(93). Lyon YA; Riggs D; Fornelli L; Compton PD; Julian RR The Ups and Downs of Repeated Cleavage and Internal Fragment Production in Top-Down Proteomics. J. Am. Soc. Mass Spectrom 2018, 29, 150–157. [PubMed: 29038993]

(94). Zenaidee MA; Lantz C; Perkins T; Jung W; Ogorzalek Loo RR; Loo JA Internal Fragments Generated by Electron Ionization Dissociation Enhance Protein Top-Down Mass Spectrometry. J. Am. Soc. Mass Spectrom, 2020 in press (10.1021/jasms.0c00160).

(95). Huang T-Y; McLuckey SA Top-down protein characterization facilitated by ion/ion reactions on a quadrupole/time of flight platform. Proteomics 2010, 10, 3577–3588. [PubMed: 20848674]

(96). Ugrin SA; English AM; Syka JEP; Bai DL; Anderson LC; Shabanowitz J; et al. Ion-Ion Proton Transfer and Parallel Ion Parking for the Analysis of Mixtures of Intact Proteins on a Modified Orbitrap Mass Analyzer. J. Am. Soc. Mass Spectrom 2019, 30, 2163. [PubMed: 31392699]

(97). Riley NM; Westphall MS; Coon JJ Activated Ion Electron Transfer Dissociation for Improved Fragmentation of Intact Proteins. Anal. Chem 2015, 87, 7109–7116. [PubMed: 26067513]

(98). Giorgetti J; Beck A; Leize-Wagner E; François Y-N Combination of intact, middle-up and bottom-up levels to characterize 7 therapeutic monoclonal antibodies by capillary electrophoresis – mass spectrometry. J. Pharm. Biomed. Anal 2020, 182, 113107. [PubMed: 32004767]

(99). Lermyte F; Dittwald P; Claesen J; Baggerman G; Sobott F; O'Connor PB; et al. MIND: A Double-Linear Model To Accurately Determine Monoisotopic Precursor Mass in High-Resolution Top-Down Proteomics. Anal. Chem 2019, 91, 10310–10319. [PubMed: 31283196]

(100). Vyatkina K; Wu S; Dekker LJM; VanDuijn MM; Liu X; Tolić N; et al. Top-down analysis of protein samples by de novo sequencing techniques. Bioinformatics 2016, 32, 2753–2759. [PubMed: 27187201]

(101). Zhou M; Gucinski AC; Boyne MT Performance metrics for evaluating system suitability in liquid chromatography—Mass spectrometry peptide mass mapping of protein therapeutics and monoclonal antibodies. mAbs. 2015, 7, 1104–1117. [PubMed: 26218711]

(102). Florio W; Tavanti A; Barnini S; Ghelardi E; Lupetti A Recent Advances and Ongoing Challenges in the Diagnosis of Microbial Infections by MALDI-TOF Mass Spectrometry. Front. Microbiol 2018, DOI: 10.3389/fmicb.2018.01097.

(103). Zhou M; Wysocki VH Surface Induced Dissociation: Dissecting Noncovalent Protein Complexes in the Gas phase. Acc. Chem. Res 2014, 47, 1010–1018. [PubMed: 24524650]

(104). Di Stefano LH; Papanastasiou D; Zubarev RA Size-Dependent Hydrogen Atom Attachment to Gas-Phase Hydrogen-Deficient Polypeptide Radical Cations. J. Am. Chem. Soc 2018, 140, 531–533. [PubMed: 29292649]

(105). Beck A; D'Atri V; Ehkirch A; Fekete S; Hernandez-Alba O; Gahoual R; et al. Cutting-edge multi-level analytical and structural characterization of antibody-drug conjugates: present and future. Expert Rev. Proteomics 2019, 16, 337–362. [PubMed: 30706723]

(106). Hernandez-Alba O; Houel S; Hessmann S; Erb S; Rabuka D; Huguet R; et al. A Case Study to Identify the Drug Conjugation Site of a Site-Specific Antibody-Drug-Conjugate Using Middle-Down Mass Spectrometry. J. Am. Soc. Mass Spectrom 2019, 30, 2419–2429. [PubMed: 31429052]

(107). Watts E; Williams JD; Miesbauer LJ; Bruncko M; Brodbelt JS Comprehensive Middle-Down Mass Spectrometry Characterization of an Antibody-Drug Conjugate by Combined Ion Activation Methods. Anal. Chem 2020, 92, 9790–9798. [PubMed: 32567851]

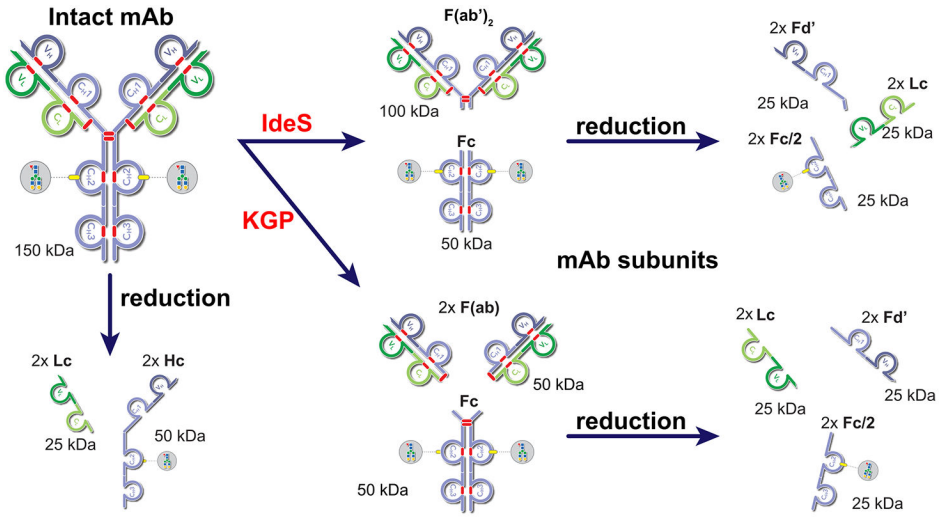

Figure 1.

Structural organization of monoclonal antibodies (mAbs) of immunoglobulins G (IgG1) type and enzymatically/chemically assisted structure-specific generation of mAb subunits (25, 50, and 100 kDa). Highly specific enzymes considered here are IdeS (FabRICATOR) and KGP (GingisKHAN).

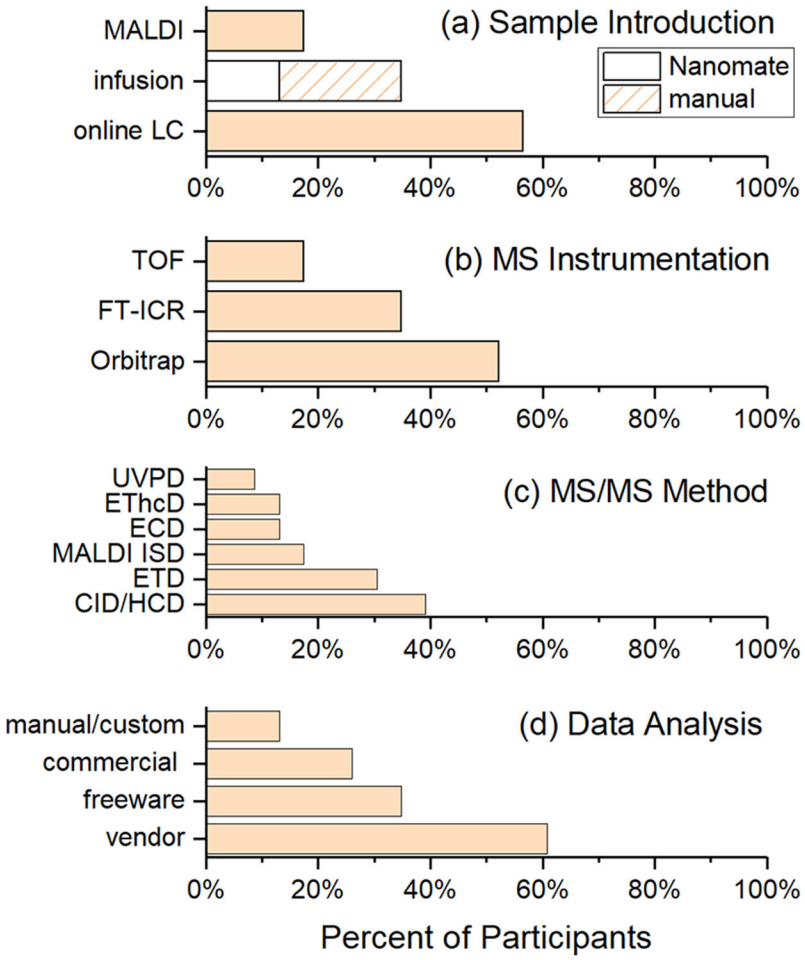

Figure 2.

Summary of the experimental methods used by the participants for TD/MD (a total of 20 participants). The percent of participants who have used specific methods for (a) sample introduction; infusion and online LC refer to ESI approaches, (b) MS instrumentation, (c) MS/MS, and (d) data analysis (where “commercial” refers to nonvendor third-party software, and “vendor” are software tools provided by the instrument manufacturers) are shown in bar graphs. Many groups used more than one method.

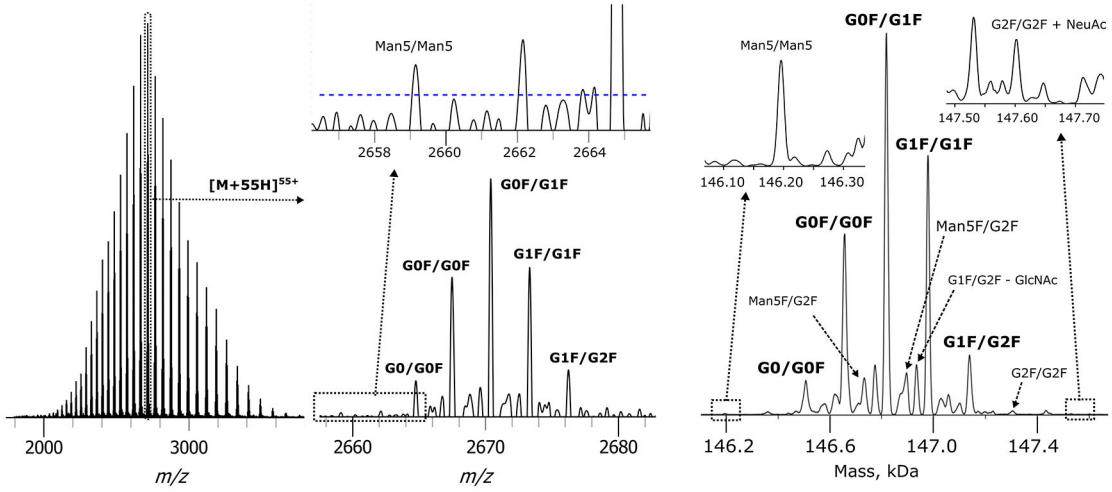

Figure 3.

Example of intact mAb average mass measurements: ESI Q Exactive HF Orbitrap FTMS of intact SiLuLite mAb (group 19). Shown are the charge state distribution (left panel), expanded view into a selected charge state (middle panel), and a deconvolved mass spectrum (right panel). Deconvolution performed by use of UniDec software. Glycoform annotation follows standard rules.[71,76] For more details and examples of experimental results, see Figures S30-S34 and Tables S8-S10.

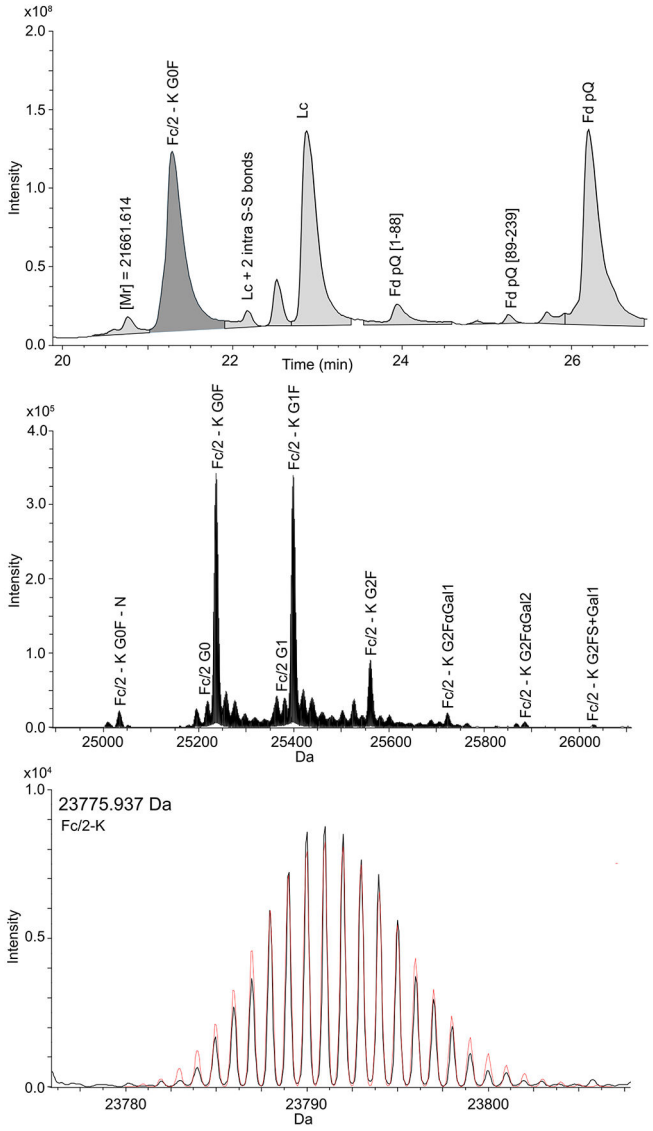

Figure 4.

MU approach examples for subunit mAb isotopically resolved mass measurements: ESI maXis II QTOF MS of 25 kDa subunits (Lc, Fd′, and Fc/2) of NIST mAb obtained by IdeS digestion and TCEP reduction of S–S bonds (group 1). Shown are (top panel) LC-MS elution profiles, with the most abundant glycoforms labeled on top of each elution peak; (middle panel) deconvolved mass measurements of glycoforms of Fc/2 subunit; and (bottom panels) example of a deconvolved baseline-resolved isotopic envelope of a glycoform Fc/2-Lys obtained with accurate isotopic distributions (calculated isotopic pattern is overlaid in red) and dynamic range spanning 2 orders of magnitude. The calculated monoisotopic mass value is given in Da. All monoisotopic neutral mass assignments were obtained by the SNAP algorithm following MaxEnt deconvolution. Proteo/glycoforms annotations are as defined in the BioPharma Compass method.[71]

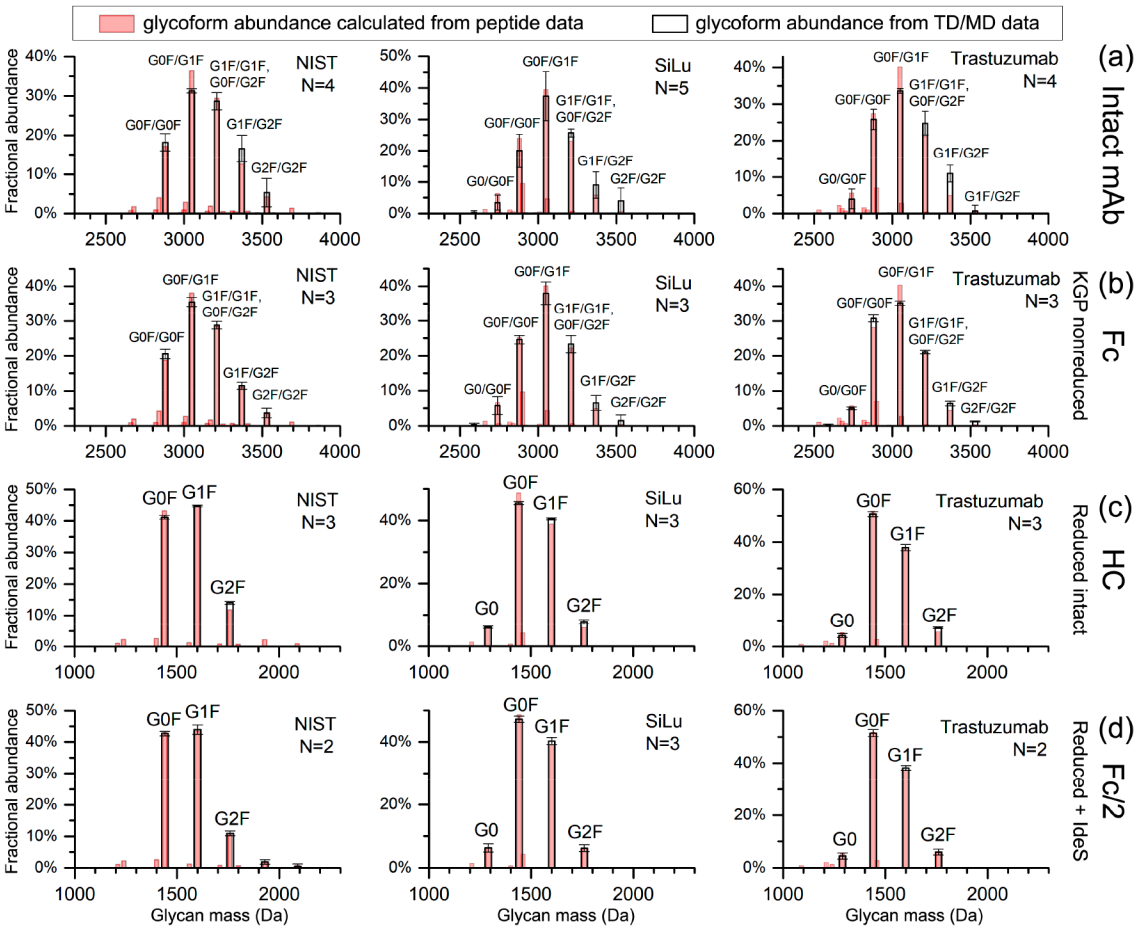

Figure 5.

Relative quantitation of major glycoforms at the (a) intact mAb level, (b) Fc from KGP digestion, (c) intact Hc after mAb reduction, and (d) Fc/2 from IdeS digestion with disulfide bond reduction for the 3 mAbs (open bars with black border). The “N” in the legend indicates the number of groups with corresponding TD/MD MS data, and the standard deviations are shown as error bars. The relative abundances were normalized to the selected major glycoforms labeled in the plots. The relative abundances from peptide mapping were overlaid as red bars, which are calculated based on the glycopeptide relative abundances of the conserved Asn300 in Fc and glycation (assuming only one glycation). For data comparison with the intact protein and the Fc region (contains two glycosylation sites) the relative abundances at the peptide level (group 16) were paired to generate a simulated profile of glycoforms assuming random combination.

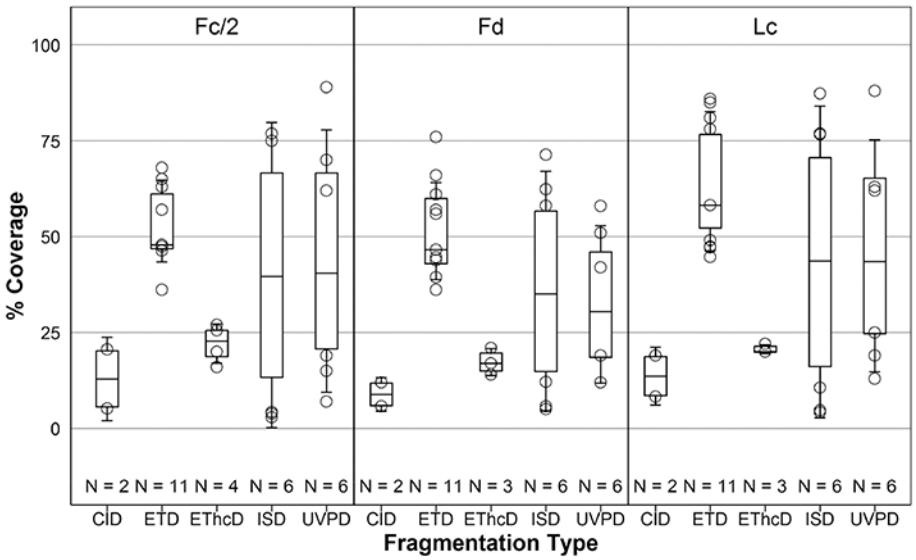

Figure 6.

Fragmentation method-classified sequence coverage in % for IdeS-digested NIST, SiLuLite, and trastuzumab mAbs obtained for disulfide bond reduced mAbs (data from all mAbs are shown together, grouped by MS/MS method and mAb subunit type). The corresponding mAb-specific data are shown in Figures S21-S23.

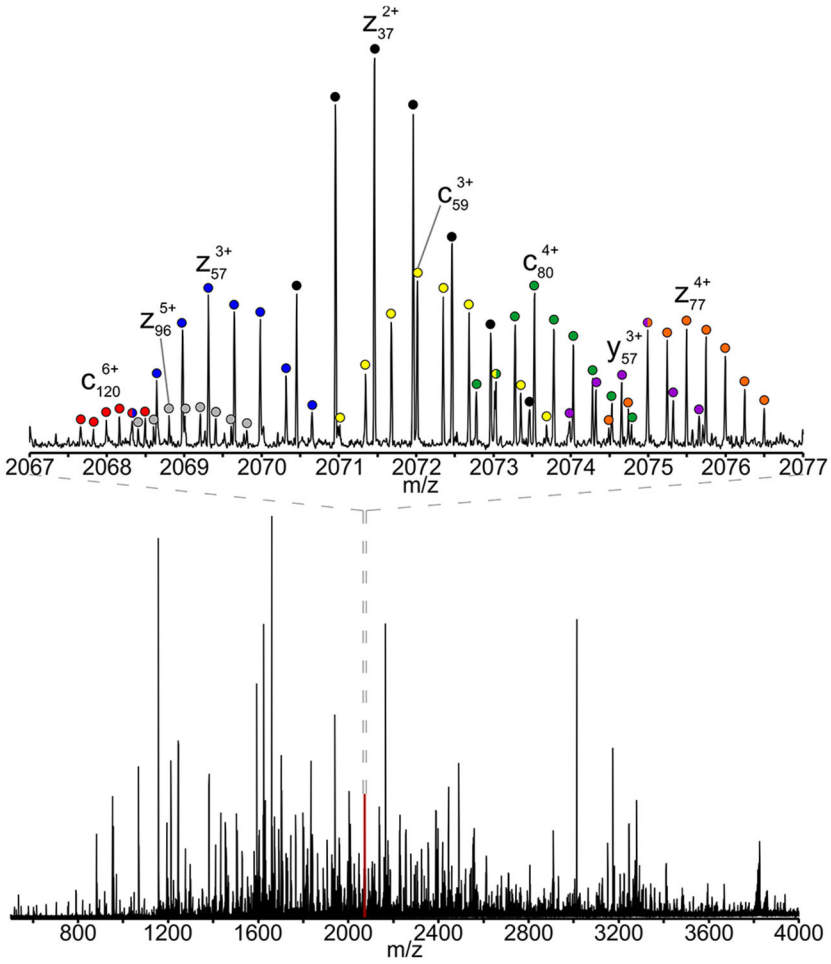

Figure 7.

Example of an MD MS application to mAb analysis: sequencing of a light chain of SiLuLite mAb with a 21 T ESI FT-ICR MS employing ETD/PTR MS/MS (group 8). The inset shows an expanded view of a tandem mass spectrum with isotopic envelopes of product ions assigned and color coded for facile visualization.

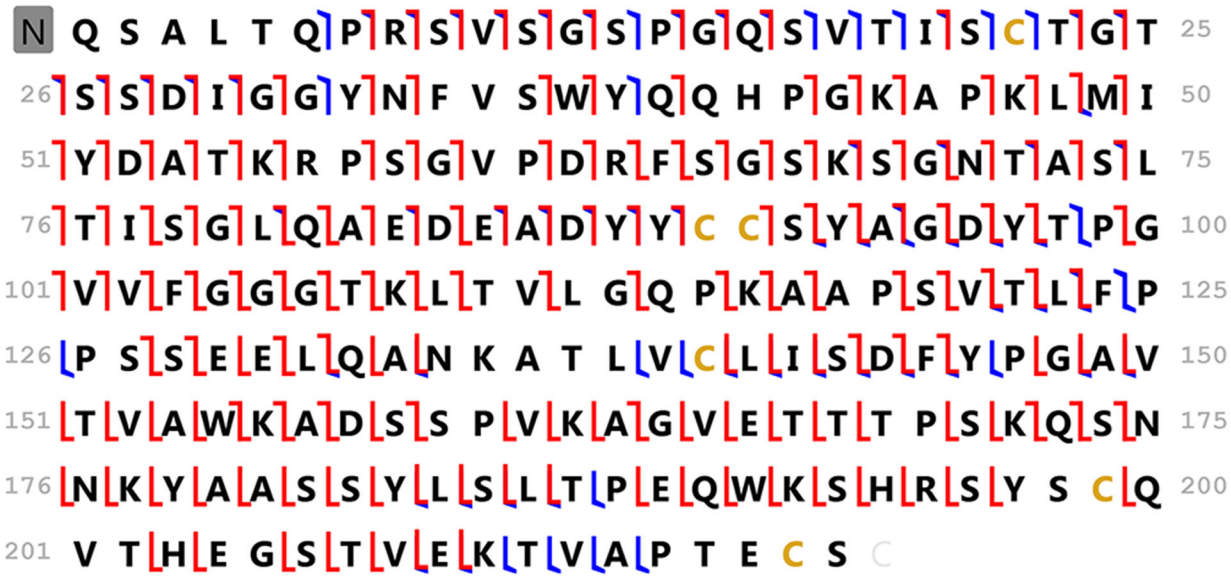

Figure 8.

Total sequence coverage of 85% achieved for the analysis of the disulfide bond-reduced light chain of SiLuLite mAb with a 21 T ESI FT-ICR MS (group 8), based on middle-down MS/MS (combination of results from two tandem mass spectra). Included are product ions identified from CID/PTR MS/MS (10 transients averaged, *b/y*-ions, cleavage sites shown in blue) and of ETD/PTR MS/MS (10 transients averaged, *c/z*-ions, cleavage sites shown in red).

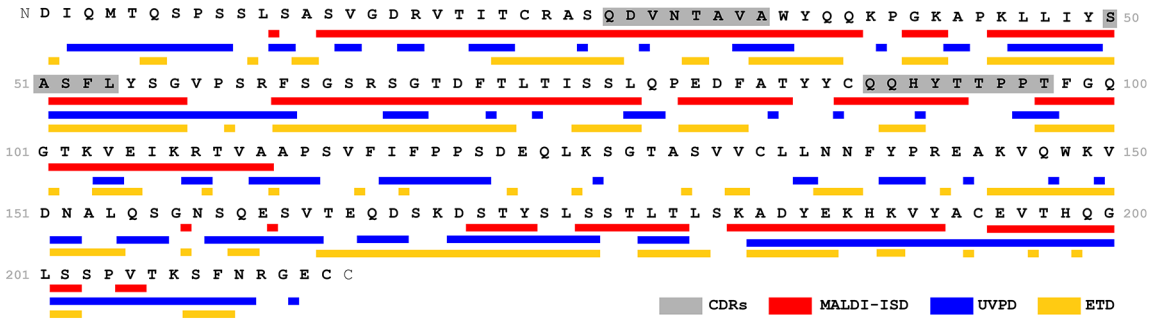

Figure 9.

Comparison of sequence coverage (represented by sequence tags) and individual backbone cleavage sites obtained with ESI UVPD, ESI ETD, and MALDI ISD MS/MS for the Lc of trastuzumab. Included data are from groups 9 (ETD), 14 (UVPD), and 21 (MALDI ISD). See Figures S35, S39, and S41 for more details.

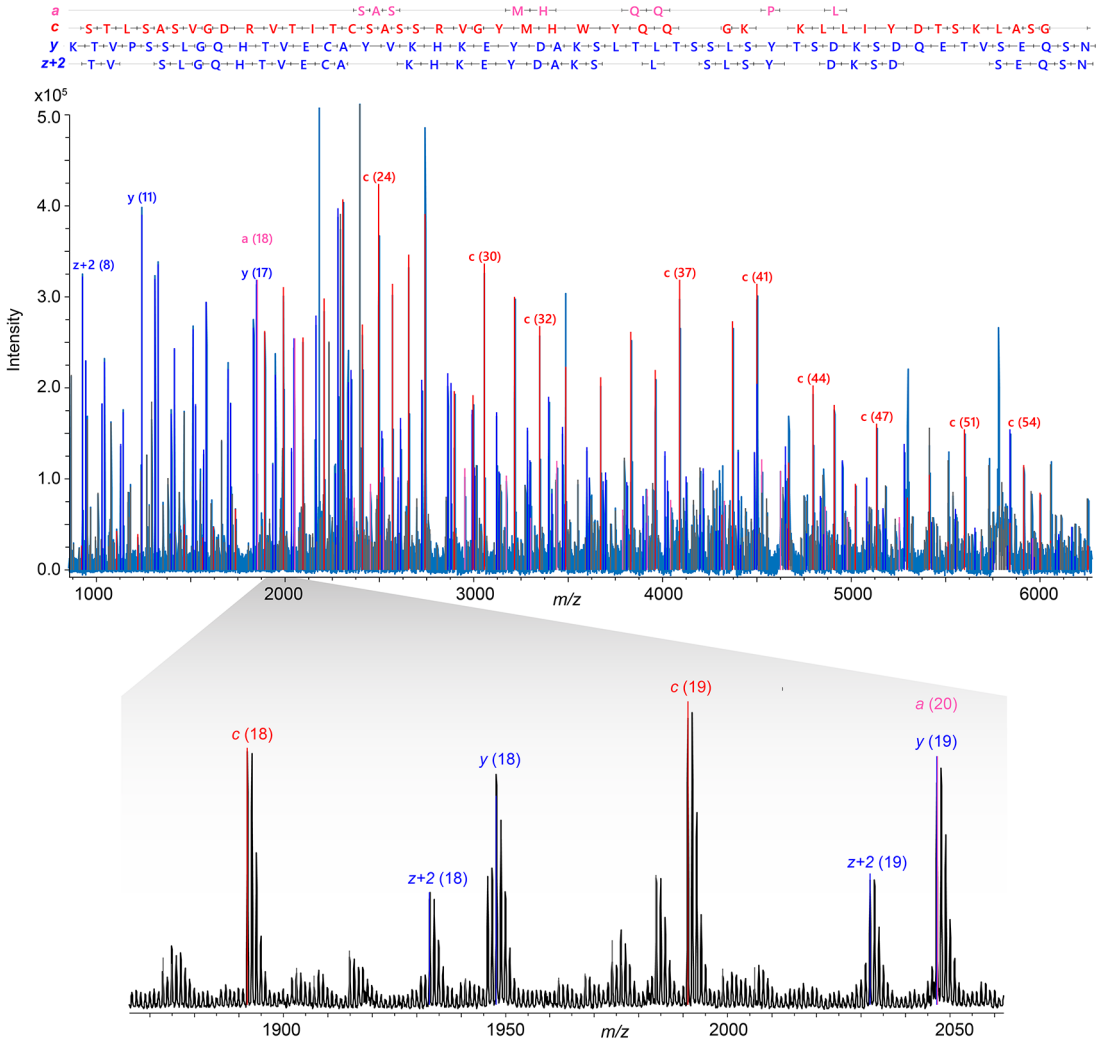

Figure 10.

Example of an MD MS mAb analysis: sequencing of the NIST mAb Lc after chromatographic separation with a Bruker rapifleX MALDI-TOF MS based on MALDI ISD MS/MS. (Top panel) MALDI ISD mass spectrum. Product ion types *a, c, y,* and $z + 2$ were assigned. Monoisotopic peak list was obtained by usage of the SNAP algorithm for singly charged ions. (Bottom panel) Expanded view of the full range mass spectrum exhibiting baseline resolution of isotopic distributions. Additional expanded views are in Figure S59.

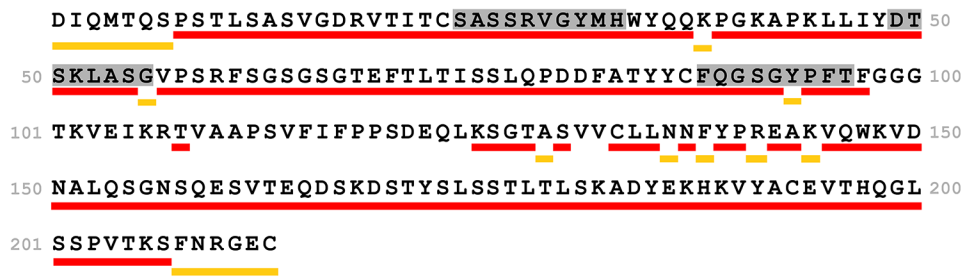

Figure 11.

Example of an MD MS application for mAb analysis: sequencing of NIST mAb Lc with a Bruker rapifleX MALDI-TOF MS based on MALDI ISD MS/MS (see Figure 10). 77% sequence coverage with matching N- and C-terminal product ions (red bricks) was obtained (CDRs are shown in gray). Yellow bricks indicate accepted gaps when sequence calculations are performed by use of the “sequence validation percentage” approach.[33]

Table 1.

Examples of the Absolute Mass Measurement Errors (Mean Value ± a Single Standard Deviation, in ppm) for Analysis of Intact mAbs and Their Subunits Generated via IdeS Digestion with and without Disulfide Bond Reduction[a]

		absolute mass measurement error (ppm)			ref
chain	**experimental details**	**FT-ICR MS**	**orbitrap FTMS**	**TOF MS**	**SI Figure**
intact	3 major glycoforms	14.9 ± 11.4	17.4 ± 19.5	35.5 ± 33.8	S1-S3
intact	G0F/G0F	11.3 ± 8.0	20.2 ± 23.2	46.1 ± 48.6	S4-S6
	G0F/G1F	17.2 ± 16.0	16.0 ± 21.7	31.9 ± 29.8	
	G1F/G1F	15.8 ± 8.6	16.0 ± 14.6	28.6 ± 26.7	
subunits (IdeS)	$F(ab')_2$ Fc	6.5 ± 7.8	4.8 ± 3.6	8.2	S13
subunits (IdeS)	all 25 kDa subunits	5.6 ± 6.7	3.3 ± 2.4	1.2 ± 0.6	S7
subunits (IdeS)	Lc/Lc pQ	6.7 ± 7.9	3.0 ± 1.8	1.1 ± 0.4	S8-S12
	Fd′/Fd′ pQ	4.1 ± 4.5	3.5 ± 2.8	1.0 ± 0.5	
	Fc/2 G0F	8.2 ± 9.3	2.7 ± 2.3	1.3 ± 0.4	
	Fc/2 G1F	4.8 ± 5.3	2.2 ± 1.7	1.3 ± 0.8	
	Fc/2 G2F	1.7 ± 0.3	6.1 ± 2.3	1.1 ± 1.0	

[a]Results are grouped by the MS platform employed: FT-ICR MS, Orbitrap FTMS, and TOF MS. Note: Table 1 reports mean values of mass measurement errors, whereas the corresponding reference figures (Figures S1-S13) report median errors.